

Design of an Underactuated Gripper with a Floating Differential Actuator

Remco de Lange and Prof. dr. ir. Martijn Wisse (Supervisor)

Delft University of Technology, Department of BioMechanical Engineering, Delft, The Netherlands

Abstract—Underactuated grippers are developed to grasp objects of varying shape and sizes without the need to rely on sensors and feedback systems. This main aspect makes underactuated grippers efficient in their ability to automatically distribute the actuation force to multiple outputs. Besides actuating multiple phalanges by the actuation principle, it is also possible to drive multiple fingers. An interesting approach is to give the actuator a spatial degree of freedom and suspend it such that it can provide its power both to the shaft as to the unconstrained degree of freedom. There already exist designs that apply this working principle to distribute a force to two and four fingers, without the need for additional differential mechanisms. In both cases the fingers are divided into two pairs, where one pair is connected to the rotor and the other to the stator. When the actuator is activated a force is transferred to the fingers connected to the rotor. The reaction force, caused by the actuation force, is acting on the stator and this force is transferred to the fingers connected to the stator. The aim of this report is to determine how the floating actuator principle can best be implemented such that the number of outputs is as high as possible.

The theoretical maximum number of outputs a floating actuator differential can achieve is seven, namely six spatial degrees of freedom and the actuated shaft. In this report it was found that it highly unlikely that this system can provide seven outputs for a sufficient workspace, due to kinematic restraints introduced by dependencies between the orientation and the position of the actuator. For the concept with a maximum of six outputs the floating actuator principle can provide ample torque for a sufficient range of motion for the fingers. The prototype, as developed in this report, shows that the floating actuator principle works for a system with six outputs.

Index Terms—Underactuated Gripper, Floating Actuator, Differential Mechanism.

I. INTRODUCTION

In the field of anthropomorphic grippers and robotic hands the principle of underactuation provides an extension of the capabilities of many grippers without the need of adding more actuators [3]. Basically the principle of underactuation entails the application of differential mechanisms to distribute forces over multiple elements of a robotic hand. These differential mechanisms also allow that the motion of each element is independent of the other elements.

Initially underactuation was primarily applied to distribute the forces over the phalanges of the finger, examples range from simple two-phalanx fingers [4]–[7] to more complex multiple-phalanx fingers [8]–[10]. The resulting fingers were capable of adjusting to the shape of the grasped object, without the need of a complex control system.

A second application of the principle of underactuation in robotic hands is to distribute the forces between the

fingers. Many conventional robotic hands use a wide variety of possible differential mechanisms, including pulley-tendon mechanisms [8,11,12], linkage-based mechanisms [13]–[17], differential gears [18,19] and compliant mechanisms [20,21]. These conventional differential mechanisms convert the single output of the actuator in multiple outputs.

An alternative concept is to suspend the actuator such that it gains one or more additional outputs. In other words, the actuator can gain an additional output when one of the Cartesian degrees of freedom (DoF's) is unconstrained [1]. Additionally the suspension can act as a differential if it is constructed in such a way that the forces are automatically distributed over the outputs of the actuator. According to our knowledge, the first application of this concept was found in the works of Meijneke et al. [1], resulting in an underactuated gripper, called Delft Hand 2.

Delft Hand 2 has three fingers with each two phalanges. One finger is directly connected to the stator of the actuator, while the other two are connected via a differential gear to the rotor of the actuator. The stator is suspended by a bearing such that it can rotate around the same axis as the rotor, giving the actuator two unconstrained DoF's. A schematic view is given in figure 1(a). The working principle of this design can be compared with a planetary differential, where the planetary gearwheel is an analogy for the magnetic field of the actuator. In other words, the magnetic field distributes the input force between a force acting on the rotor and an equal force in opposite direction acting on the stator. Experiments have shown that the concept can result in a functional and reliable underactuated gripper [1].

In order to establish a firm grip on an object one requires at least seven contact points on important locations [22], assuming there is no friction. For this reason Delft Hand 2 has three fingers, despite that the actuator only has two outputs. As mentioned, a differential gear is used to obtain the third output. The third output can also be obtained by unconstraining another DoF. An exemplary design with four unconstrained DoF's is known as Abel's hand [2].

Abel's hand consists out of four fingers with each having only one phalanx. Two fingers are connected to the stator and the other two are connected to the rotor. In the case of Abel's hand, figure 1(b), two additional DoF's are required, namely the horizontal displacement perpendicular to the axle of the actuator and the rotation of the actuator around the vertical Cartesian axis. These two DoF's allow for a behavior on both sides of the actuator that is similar to the functioning of a two-dimensional linkage-based differential, namely the Whippletree.

Experiments have shown that the actuator in Abel's hand works as a differential with four outputs and is able to distribute the input force almost equally over the four fingers [2].

When extending on the concept of using unconstrained DoF's of the stator of the actuator, then it is theoretically possible to obtain an actuator that can act as a differential mechanism with seven outputs. For a schematic impression see figure 1(c). As far as we can investigate such mechanism has not been developed.

A. Objective

The goal of this research is to investigate the maximum number of spatial degrees of freedom of the actuator can be used, such that the actuator can act as a differential and distribute the forces between the fingers of a gripper. In order to provide the proof of concept the secondary goal is to design and build a prototype.

B. Outline

In section II the working principle is discussed and explained, which lead to a minimal set of criteria. From these criteria several conceptual designs are proposed. Section III assesses the workspaces of each of the proposed designs, which leads to the selection of the most promising concept. In section IV an assessment and optimization are performed to obtain the largest possible minimal output torque for the entire workspace, while ignoring the effects of gravity on the concept. Section V continues with the best dimensions for the concept found in section IV and analyses the influence of gravity on the design. In section VI the results found in section V are converted in a prototype design. And experiments are performed to investigate the performance of the prototype. This is followed by section

VII, discussing the results found in this report. Finally the conclusions are drawn in section VIII.

II. CONCEPTUAL DESIGN

As mentioned in the previous section, the goal of this thesis is to develop an underactuated gripper that is capable of distributing the output force over as many fingers as possible, without the need for an additional differential mechanism. In other words, the suspension of the actuator and the connection of the actuator to the fingers must be able to incorporate differential properties. When the suspension mechanism of an actuator allows for more than one output, then we will refer to that system as a *differential actuator*. In this section the working principle and criteria are discussed. Based on both the working principle and the criteria, the most relevant concepts are proposed.

A. Design Choice

For this investigation the fingers are divided in two pairs, each consisting of three fingers, which are placed opposite of each other. The reason for placing the pairs of fingers opposite of each other is that the most commonly used grasps, by a person during an average day in a residential environment, requires at least two opposing fingers [23]. Additionally it seems that this is the most common design choice when building grippers [1,4,7]. And even for anthropomorphic hands the aim is to often have an opposable thumb [5,12]. Additionally each of the fingers is positioned such that the axis of each of the revolute joints has the same orientation.

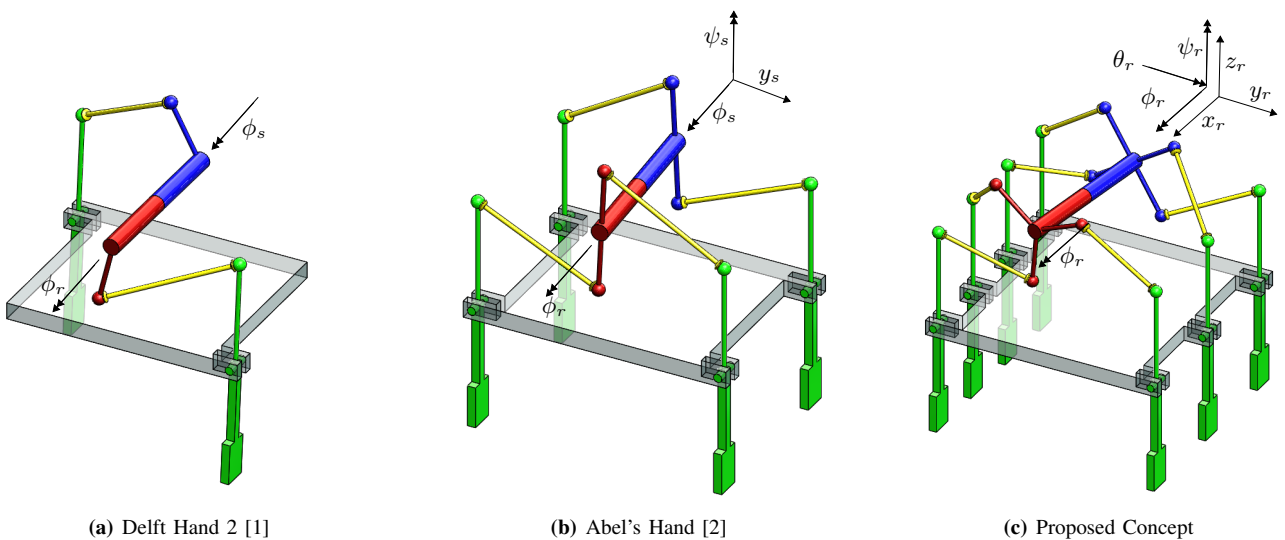


Figure 1. In each figure the stator and the rotor of the actuator are depicted respectively in blue and red. Each of the fingers (green) is connected by a rigid mechanical component (yellow) to the actuator. The differential function of the actuator requires the actuator to have several unconstrained degrees of freedom, indicated by the black arrows and denoted by $_s$. The actuated degree of freedom is denoted by $_r$. In the case of Delft Hand 2, figure 1(a), the rotation of the actuator's stator is the additional unconstrained DoF. Note that the rotation is parallel to that of the rotor. In the case of Abel's hand, figure 1(b), two additional DoF's are required, namely the horizontal displacement perpendicular to the axle of the actuator and the rotation of the actuator around the vertical axis. The actuator in Abel's hand works as a differential with four outputs. Figure 1(c) depicts the concept where all the DoF's are used, resulting in a differential mechanism with seven outputs.

B. Design Components

Each system with a differential actuator requires four components and a set of joints which connect these components. Each of these components has a specific function.

1) *Frame*: The function of the frame is to fixate the positions of each of the fingers relative to each other. Additionally the frame can act as a plane to which the fingers can push the grasped object to obtain a firmer grip. The joint connecting the frame to the finger should provide each finger with only one degree of freedom. Generally this will be a revolute joint.

2) *Fingers*: The function of the fingers is to obtain contact with the grasped object by moving inward. In order to obtain a firm grip, the fingers need to transfer the input force, received from the linkage to which each finger is connected, onto the grasped object.

3) *Linkages*: The main purpose of the linkages is to connect the actuator with each of the fingers, such that a kinematic solution exists. This connection is required to transfer the output power of the actuator to each of the fingers. Subsequently the linkages must be able to add a constraint on the actuator when the corresponding finger is obstructed to move by the grasped object. The joints between the linkage and both the actuator and the fingers must not constrain the movement of these components. For the simpler cases, such as depicted in figure 1(a), a one-DoF joint can be sufficient, but for more complex systems two- or three-DoF joints might be required.

4) *Actuator*: The main purpose of the actuator is to provide an actuation torque or force to the connected linkages. The actuator is connected to linkages which transfer the output force to the fingers. In order for the actuator to act as a differential actuator at least two linkages must be connected and the actuator must have at least one spatial DoF. Normally the linkages are connected to the rotor of the actuator, but for this concept it can be better to connect one or more linkages to the stator.

C. Working Principle

The working principle of the differential actuator requires that the actuator has one DoF in Cartesian space for each additional output. Figure 1 shows three examples of differential actuators with an increasing number of outputs.

An example with two outputs is given in figure 1(a), here the stator of the actuator can rotate around the same axis as the rotor and is connected to a second finger [1]. Obviously the rotor is connected to the first finger. Assume that a torque is applied by the actuator then the desired behavior would be that both fingers move inwards, until they both touch the object to grasp. The finger that touches the object first experiences more resistance, slowing it down or even stopping it completely. Allowing the other finger to catch up and touch the object as well. When the finger connected to the rotor is the first to touch the object then only the stator can rotate. This means that the actuator as a whole rotates relative to the global coordinates, i.e. it uses one of the Cartesian DoF's.

A more complex example is given in figure 1(b) and has four fingers, requiring two additional DoF's [2]. Two fingers are connected to the stator and the other two are connected

to the rotor. When all the fingers have the same inward displacement, then this system basically behaves similar to the previous example. In other words, in this specific situation it uses the same DoF's. As soon as one finger touches the object, a constraint is added to the system. This is effectively establishing a relation between two DoF's, and thereby resulting in a displacement or rotation of the actuator in one of the two additional DoF's or a combination of both. For example, assume that both fingers on one side of the actuator touch the object. Then the rotation around the vertical axis is constrained and the actuator has to move perpendicular to the actuated axis.

Generalized this means that for any arbitrary set of fingers touching the object, there must exist a combination of DoF's such that the remaining set of fingers are still able to move further inwards. This means that the actuator needs to be able to facilitate this continued movement by translating and/or rotating itself.

This working principle allows for a maximum of seven fingers to be actuated by a differential actuator. This number is limited because each finger requires one DoF and the maximum number of DoF's that a differential actuator can have is seven. These DoF's are the six spatial DoF's supplemented with the actuated DoF of the actuator. Figure 1(c) shows an example of a differential actuator that is connected to the maximum number of fingers.

D. Concept Criteria

In order to ensure that the concept behaves according to the working principle described in section II-C, the concept has to comply with at least the first three criteria. A fourth criterion has been determined during the literature survey. This survey investigated the conventional differential mechanisms, which could form a base for a differential actuator. It was found that the linkage-based differentials provided the best base. Combined the concept has to comply with the following four criteria:

- The actuator must have at least the same number of DoF's as the number of fingers.
- Each finger must be able to move over the entire range independent of the other fingers.
- The direction of the force applied on the finger must be the same for any possible configuration.
- The connection between the actuator and the finger must be a rigid linkage with on either side a joint.

E. Concepts

The characteristics which define a concept are the type of actuator, the number of fingers and the combination of which fingers are connected to the stator and which are connected to the rotor. For this section a division is made solely on the type of actuator and the number of fingers, resulting in several concepts.

For each number of fingers can in theory be actuated by either a rotary actuator or a linear actuator. Therefore for each number of fingers the concepts can be divided into two groups. The concept for a rotary actuated concept with the theoretical maximum amount of seven fingers is depicted in 2(a).

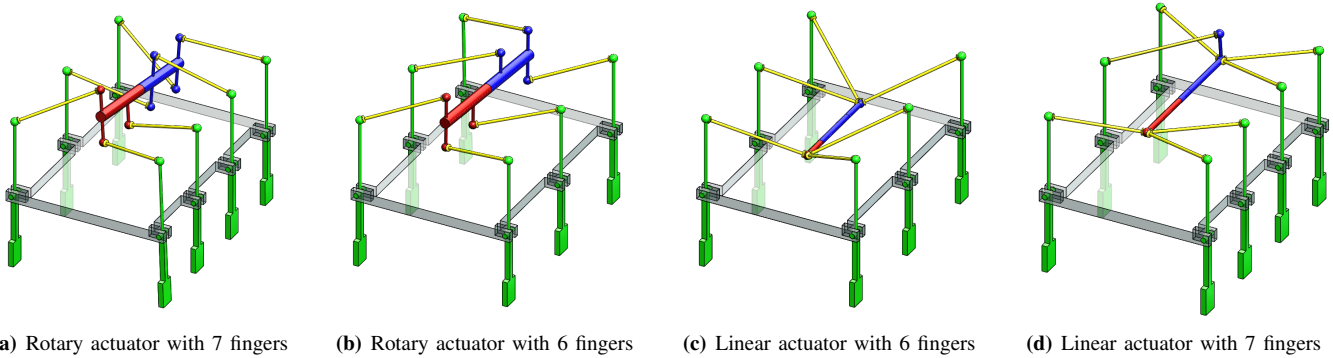


Figure 2. Concepts of different solutions for differential actuators with six or more outputs. In each figure the stator and the rotor, or pushrod, of the actuator are depicted respectively in blue and red. Each of the fingers (green) is connected by a rigid mechanical component (yellow) to the actuator.

An obvious alternative would be to connect a linear actuator to seven fingers, as depicted in figure 2(d). Though the seventh finger has to be connected with an offset from the working axis, to establish a relation with the rotation around the axis of the actuator, which is the seventh DoF. Because it is a linear actuator, it is apparent that the actuator cannot apply a torque around the working axle. This means that there can only be a torque equilibrium around the working axle when the component of the force perpendicular to the working axle, and exerted by the linkage, is zero. Assume that object exerts a force on the finger, resulting in a force exerted by the linkage larger than zero. Then there can only be an equilibrium when the linkage lies in the plane spanned by the three points where the actuator is connected to the linkages. Otherwise the actuator will rotate either until the perpendicular component of the force exerted by the linkage will become zero or until the entire force becomes zero. In the case that the entire force is zero it is apparent that the seventh finger is redundant. In the other case the rotation around the actuator remains unconstrained, which implies that there are more constraints than there are other degrees of freedom. As a result the remaining system is overdetermined, which is undesirable.

As a direct consequence the only viable solution is to remove the seventh finger. This results in a concept that is driven by a linear actuator and has six fingers, as depicted in 2(c). Note that this is technically an underdetermined system, because the rotation of the linear actuator around his working axis is not constrained in any way.

In order to make a fair comparison between the effects of a linear actuator and a rotary actuator, a concept, as depicted in figure 2(b), is added. This concept has six fingers and a rotary actuator, and is also an underdetermined system.

In case none of the concepts provide satisfactory results, then it might be possible to assess the concepts with five fingers in a later stage in this research. Note that other researcher already provided proof that it is possible to have a differential actuator with four fingers/outputs [2].

F. Conclusion

Based on the working principle it became apparent that the theoretical maximum number of outputs that can be actuated by

a single differential actuator is seven. Therefore it is possible to propose a concept with seven fingers and a rotary actuator. Unfortunately it proved to be impossible to actuate seven fingers with a linear actuator, which led to the alternative of a concept with six fingers and a linear actuator. Finally a concept with six fingers and a rotary actuator was added, in order to allow for a fair comparison between the effects of a rotary and a linear actuator.

III. KINEMATIC WORKSPACE

In section II, three concepts were introduced. Each of the concepts is a closed-loop parallel mechanism, and therefore is similar to a Stewart-Gough platform, i.e. the actuator serves as the platform. For these systems it is known that the closed-loop nature of parallel mechanisms limits the motion of the platform and can create complex kinematic constraints inside the workspace [24]. Therefore it is essential to gain insight about the constraints which could occur within the desired workspace for each of the given concepts. In this section a kinematic analysis described and the results are discussed. Based on these results the most promising concept is determined.

A. Method

The aim of the analytical model is to determine whether there exists a kinematic solution for each point in the required workspace. For this particular system it is best to describe the workspace by a range of motion for each of the fingers. This implies that the input for the analytical model is a set of angles for the fingers and that the output is the position and orientation of both the housing and the axle of the actuator.

For each concept, the system is a complex spatial constraint problem and unfortunately it is not possible to find an algebraic solution for each of them. Only for the concept with six fingers and a linear actuator it is possible to find an algebraic solution. The primary concern with a non-algebraic solution is that one cannot be certain that a solution does not exist when the numerical solver does not produce a solution. Therefore two methods are implemented, one numerical method for the concepts with rotational actuators and one algebraic method for the concept with the linear actuator.

1) *The general approach:* is to find an initial kinematic solution for the initial configuration, where all the fingers are in the vertical orientation. This orientation is defined as an angle ϕ_j of 0 degrees, where j indicates the finger. From this point each of the fingers is rotated incrementally and independent from each other, over a range from -20 to +20 degrees. In case no significant differences are found between the concepts, then the range will be increased. For each step a kinematic solution has to be found which does not differ too much from the previous solution. If such solution is not found, then the previous inputs are considered to be the boundary of the workspace.

This discrete approach consistently investigates an increasing workspace around the chosen starting configuration. The resulting workspace has the same number of dimensions as the concept has fingers. Though each workspace is only an indication for the specific dimensions for which the analysis is performed. Therefore dimensions are altered if the actual workspace is smaller than the required workspace. The dimensions which are modified are the lengths of the linkages and the lengths of the fingers.

2) *The numerical method:* The first step in the numerical method is to determine the position of the joint between the linkage and the finger, denoted by \mathbf{f}_j . Equation III.1 describes a rotation around the global x-axis and gives the relation between the length of the finger, $l_{f,j}$, the center of rotation, $\mathbf{x}_{f,j}$, and the angle ϕ_j .

$$\mathbf{f}_j = \mathbf{R}_x(\phi_j)\mathbf{l}_{f,j} + \mathbf{x}_{f,j} \quad (\text{III.1})$$

The second step is to find a solution to the constraint problem which describes how the actuator is connected to all the joints with the fingers. Note that the actuator is split in two parts, namely the housing and the axle of the actuator. The parameters referring to these parts are indicated by i , where $i = 0$ is referring to the housing and $i = 1$ to the axle. Combined with the choice to describe the orientation by quaternions this results in a system with seven parameters per part, namely the position \mathbf{x}_i and the orientation \mathbf{q}_i . The linkage between the finger and a part of the actuator is described by a distance constraint, as in equation III.2.

$$\|\mathbf{R}(\mathbf{q}_i)\mathbf{p}_{i,j} + \mathbf{x}_i - \mathbf{f}_j\| - l_j = 0 \quad (\text{III.2})$$

Equation III.2 is added for each connection between the actuator and a finger. Here $\mathbf{R}(\mathbf{q}_i)$ is the rotation matrix of either the housing or the axle of the actuator and $\mathbf{p}_{i,j}$ is the offset of the joint, between the actuator and the linkage, relative to the center of the part of the actuator, which is indicated by \mathbf{x}_i . The parameter l_j refers to the length of linkage that connects the actuator to the finger.

The housing and the axle of actuator can only rotate relative to each other around their local x-axis. This is described by a set of equations, see equation III.3, for constraining the relative rotations, around the local y-axis and z-axis of the actuator. Equation III.3 calculates whether both the y-axis and the z-axis of the axle are perpendicular to the x-axis of the housing. If this is the case then the dot-product between those vectors equals one.

$$\mathbf{R}(\mathbf{q}_1) \begin{pmatrix} 1 \\ 0 \\ 0 \end{pmatrix} \cdot \mathbf{R}(\mathbf{q}_2) \begin{pmatrix} 0 \\ 1 \\ 0 \end{pmatrix} - 1 = 0 \quad (\text{III.3a})$$

$$\mathbf{R}(\mathbf{q}_1) \begin{pmatrix} 1 \\ 0 \\ 0 \end{pmatrix} \cdot \mathbf{R}(\mathbf{q}_2) \begin{pmatrix} 0 \\ 0 \\ 1 \end{pmatrix} - 1 = 0 \quad (\text{III.3b})$$

Additionally the distance between the housing and the axle remains constant, which can be described by a set of distance constraints, see equation III.4.

$$\mathbf{R}(\mathbf{q}_1)\mathbf{p}_{a,1} + \mathbf{x}_1 - \mathbf{R}(\mathbf{q}_2)\mathbf{p}_{a,2} + \mathbf{x}_2 = \mathbf{0} \quad (\text{III.4})$$

Here $\mathbf{p}_{a,i}$ is the position of the joint relative to the center of the actuator part, \mathbf{x}_i .

Because the system is described by quaternions the following constraint, see equation III.5, has to be added. This equation ensures that the quaternion is properly represented by a unit-vector.

$$\|\mathbf{q}_i\| = 1 \quad (\text{III.5})$$

Note that for the 7-DoF rotary concept the constraint problem will be completely defined, but for the 6-DoF rotary concept it will be an under-defined constraint problem.

The final step in the numerical method is to apply the Newton solver to find a solution for the constraint problem.

3) *The algebraic method:* is specifically tailored for the concept with six fingers and a linear actuator. The main difference between this concept and the rotary concepts is that the joints between the actuator and the linkages are concentrated in two points. One point is positioned on the housing and the other on the shaft of the actuator. Because this is a static analysis, it is therefore possible to further simplify the equations by defining the joint position as the center of the corresponding actuator part \mathbf{x}_i .

The resulting problem is best described as two triangulation problems. For each part of the actuator it is possible to describe a pyramid, see figure 3. Note that nature of the problem highly depends on the design choice to connect three fingers to each of the actuator parts.

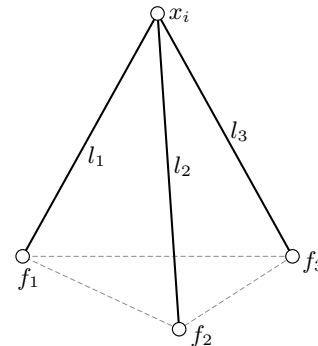


Figure 3. The triangulation problem for which the apex x_i needs to be found. The linkages have a length, l_j , which determines the distance between a base point, f_j , and the apex. The base points are the points where the linkages are connected to the fingers. Note that a second solution exists, this solution is the symmetric solution on the other side of the base.

For both triangulation problems the following steps need to be performed. First the points spanning the base of the pyramid, f_j , need to be determined. These points are the same as the joints between the linkages and the fingers and can therefore be calculated by equation III.1.

The second step is to determine the apex of the triangular pyramid as depicted in figure 3. The position of the apex can be found by solving a set of equations, where each equation describes the distance between the apex and a base point, as in equation III.6. Here that l_i are the lengths of the linkages.

$$\|\mathbf{x}_i - \mathbf{f}_j\| - l_j = 0 \quad (\text{III.6})$$

For equations III.6 it is always possible to find two solutions each on one side of the base of the pyramid. Both solutions are viable and it is a design choice to determine which of both is most suitable. It is essential that this choice is consistent during the optimization process. In case a kinematic solution is not possible, then the numerical solution will have an imaginary part. This property will be used to determine whether a kinematic solution exists.

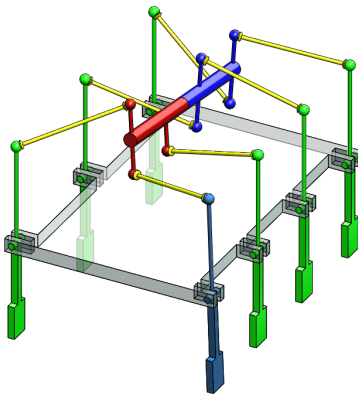
B. Results

The results of the kinematic analyses show a large difference in possible workspaces between the concepts with a rotary actuator and those with a linear actuator. For the concepts with a rotary actuator relatively small workspaces were found, compared to the concept with a linear actuator.

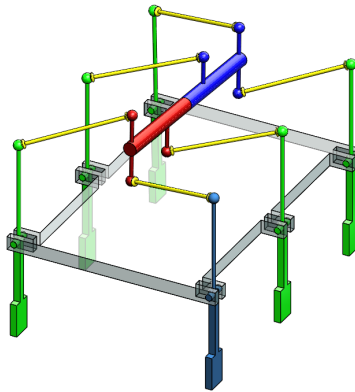
In the case of the rotary actuator, the limitations on the workspace primarily occurred when a majority of the fingers already made contact with the object to grasp. In these situations the remaining fingers were often limited to move in a small to infinitesimally small interval of its required range.

The results show that the concept driven by a linear actuator is capable of encompassing the entire required workspace. But only when the lengths of the linkages are long enough, such that the linkages can reach each other. An example of a part of the workspace is depicted in figure 4(f).

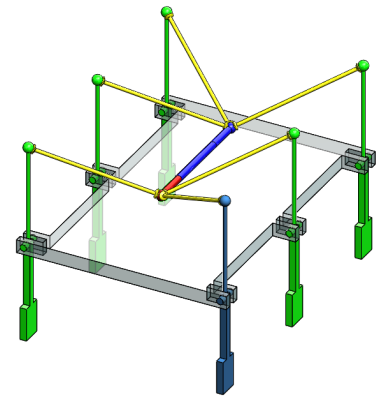
On the other hand the results for the grippers driven by a rotary actuator show that these grippers are not capable of encompassing the entire required workspace. For the specific case where all fingers are moved simultaneously with the same increment, each finger is able to reach the outer edges of the



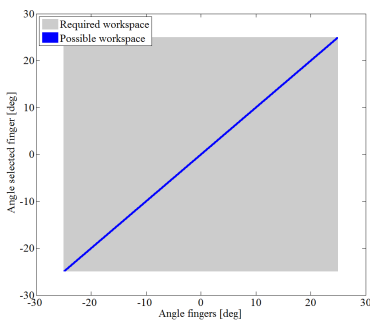
(a) Rotary actuator with 7 fingers



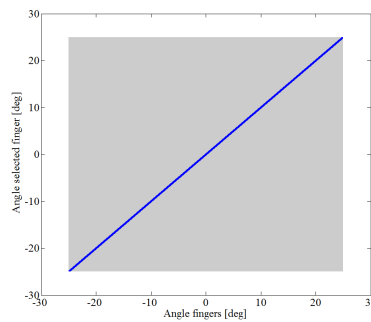
(b) Rotary actuator with 6 fingers



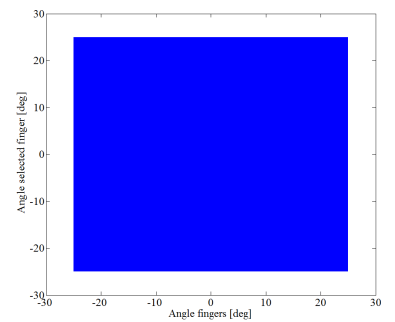
(c) Linear actuator with 6 fingers



(d) Workspace for rotary actuator with 7 fingers



(e) Workspace for rotary actuator with 6 fingers



(f) Workspace for linear actuator with 6 fingers

Figure 4. Kinematic solutions for the given angles of the fingers. Note that for simplicity this figure only shows one variation of the fingers. In this case the angle of the selected finger is varied independently from the other fingers. Figures 4(a), 4(b) and 4(c) show the three concept categories. In each of these figures the stator and the rotor of the actuator are depicted respectively in blue and red. Each of the fingers (green) is connected by a rigid mechanical component (yellow) to the actuator. The selected finger that moves independently from the other fingers is highlighted in dark blue. Figures 4(d), 4(e) and 4(f) show the respective results, where the angle of the independent finger is on the vertical axis and the angle of the other fingers is on the horizontal axis. The grey area indicates the required workspace for which a kinematic solution should exist and the blue area indicates the configurations for which a kinematic solution is found. Figures 4(d) and 4(e) show that kinematic solutions are only found when the angle of the selected finger is approximately equal to the angle of the other fingers, while figure 4(f) shows that kinematic solutions for any combination of angles exist.

required workspace. Though generally for most configurations the fingers are restrained to move independently inside a local range smaller than one degree, as can be seen in the workspaces depicted in figures 4(d) and 4(e).

Overall the results show that the rotary driven concepts have relatively small workspaces, compared to the linear driven concepts.

C. Discussion

To gain insight into why the motion is limited for the concepts with a rotary actuator, consider the following simplified case. Assume that there is one remaining finger, which does not touch the object. Then there exist two trajectories that need to line up, in order to allow the remaining finger to move. The first trajectory is the path that the actuator can follow as a result of the constraints imposed by the other fingers. The second trajectory or set of trajectories, are introduced by the linkage between the actuator and the remaining finger. Each specific configuration has an unique set of trajectories. Apparently for the rotary actuator these two trajectories often do not line up.

The question remains why this occurs more often for a rotary actuator than for the linear actuator. And the answer is related to the fact that the orientation of the actuator around the actuated axis is irrelevant in the case of the linear actuator. In this situation it is possible to focus on the plane perpendicular to the actuated axis, for which equation III.7 needs to be satisfied.

$$\delta \mathbf{x}_{joint} = \delta \mathbf{x}_{actuator} + \delta \mathbf{R}(\mathbf{q}_{actuator}) \mathbf{p}_{joint} \quad (\text{III.7})$$

Here the change of the position of a joint $\delta \mathbf{x}_{joint}$ at an offset \mathbf{p}_{joint} from center of the actuator $\mathbf{x}_{actuator}$, depends both on the displacement $\delta \mathbf{x}_{actuator}$ and the change in orientation $\delta \mathbf{R}(\mathbf{q}_{actuator})$ of the actuator. In the case of the linear actuator the offset is zero, thereby reducing equation III.7 to equation III.8.

$$\delta \mathbf{x}_{joint} = \delta \mathbf{x}_{actuator} \quad (\text{III.8})$$

Consider that this simplification is applicable on all the connections of the fingers with linear actuator. This results in a less complex set of constraint equations, which consequently leads to better results in the workspace analyses.

D. Conclusion

The relatively small workspaces found for the concepts with a rotary actuator, as described in section III-B, led to the selection of the linear actuator with six fingers as the final concept category. This conclusion is based on us not being able to find a design, during the workspace analyses, which complied with the criterion that all the fingers should be able to move independent from the other fingers for their entire range of motion. It is important to note that workspace analyses are dimension and case specific [24]. Therefore we cannot conclude that a design for a rotary differential actuator, which complies with the criteria, does not exist. Instead we conclude that the linear actuator with six fingers has the most potential.

IV. TORQUE OPTIMIZATION WITHOUT GRAVITY

In section III, the kinematic analysis showed that a kinematic solution for the entire workspace was found only for the concept with six fingers and a linear actuator. The primary criterion for the kinematic solution was that each of the fingers of the gripper is capable of moving independently from each other.

In this section an investigation is made about optimizing the torques, which the actuation mechanism distributes to the fingers. Besides the desire to obtain maximum output torques with a minimal input force, it is more important that the output torque is always in the desired direction. Otherwise it might occur that at least one of the fingers will not make a grasping motion. Overall this section will provide a set of dimensions for which the concept performs optimally, and will give insight in the effects of these parameters on the torque output.

A. Method

An analytical model of the concept is implemented in Matlab in order to determine the output torques applied on the fingers by the actuator. The analytical model investigates the entire required workspace and determines in the first stage whether or not a kinematic solution can be found for each relevant set of angles of the fingers. If a kinematic solution exists then the force transfer is determined in order to find the torques on the fingers imposed by the actuator. Note that the calculation of the kinematics is exactly the same as the analytical model described in section III-A or more specifically in section III-A3.

1) *Force transfer:* When the kinematic calculation finds a solution then the apexes of two pyramids are found, which are denoted by x_i , where $i = 1, 2$. The line along which the output force, F_{act} , of the linear actuator will act is given by the two apexes. For each apex the force equilibrium as described in equation IV.1 must hold.

$$F_{l_1} \hat{\mathbf{v}}_1 + F_{l_2} \hat{\mathbf{v}}_2 + F_{l_3} \hat{\mathbf{v}}_3 - F_{act} \frac{\mathbf{x}_1 - \mathbf{x}_2}{\|\mathbf{x}_1 - \mathbf{x}_2\|} = \mathbf{0} \quad (\text{IV.1})$$

Here $\hat{\mathbf{v}}_j$ are the normalized vectors which indicate the direction of the force in linkages, $F_{l,j}$, for each of the fingers j , which are connected to the corresponding apex. These normalized vectors are given by equation IV.2.

$$\hat{\mathbf{v}}_j = \frac{\mathbf{f}_j - \mathbf{x}_i}{l_j} \quad (\text{IV.2})$$

The forces in the linkages, $F_{l,j}$, are now known and can be converted to a force perpendicular to the finger and parallel to the xz -plane. Multiplying this force with the length of the corresponding finger gives the torque applied by the actuator on the finger, see equation IV.3.

$$T_j = (F_{l,j} \hat{\mathbf{v}}_{j,x} \sin \phi_j + F_{l,j} \hat{\mathbf{v}}_{j,z} \cos \phi_j) l_{f_i} \quad (\text{IV.3})$$

Note that this model considers only the static cases for which it is assumed that the output torques and the contact forces of the object on the fingers are in equilibrium. And that the contact forces are not calculated in this analysis and are instead assumed to apply a torque equal and opposite to the actuation torque. Another simplification for this model is that the gravity and mass are neglected.

2) *Optimization*: The goal of the optimization is to find a set of parameters for which the gripper performs optimally. For this case we define optimal when the gripper has the largest workspace for which the following criteria hold on each interval within the workspace:

- A kinematic solution exists.
- The torques on each of the fingers are in the right direction.
- The magnitudes of all the torques are larger than the minimal required torque, T_{min} .

When all criteria are met the cost value, q_{cost} , is reduced with 1. The resulting cost function is given in equation IV.4 and gives a percentage of the required workspace that complies with the aforementioned criteria.

$$Q = \frac{q_{cost}}{n} \quad (IV.4)$$

The optimization algorithm which is used is a standard method implemented in Matlab and is known as *fminsearch*. This method finds the minimum value for an unconstrained multivariable function and is a derivative-free method. In the first step the optimization algorithm tries to find the optimal values for the lengths of the linkages, l_i and for the lengths of the fingers, l_{f_i} . For the first step the minimal required torque has a magnitude of 0 Nm. When an optimal solution is found then the minimal required torque, T_{min} , is gradually increased and the optimization is repeated. The repetition continues until the optimization method can no longer find a solution for which the criteria for the cost function are met for the entire workspace.

Note that the optimization process focuses on the minimal torque which can be found on one of the fingers for any position within the workspace. The minimal torque is important because it is necessary to ensure that a minimal torque is always applied on any finger. Nonetheless this minimal torque probably is not a good measure for the average torque. Therefore the average torque and maximum torques will only be determined to gain better insight in the overall performance of the optimal configuration.

3) *Design parameters*: The optimization method determines the lengths of both the linkages and the fingers. But the concept is described by more parameters. These design parameters are not determined by the optimization process, but their influence is assessed individually. The reason for this is that these parameters cannot always be chosen optimally, because they can be limited by design choices. Additionally, by adding a design parameter in the optimization process the cost function, Q , might need to incorporate bounds on the design parameter. This will most probably lead to more local minima and the dependency of weight factors. In general these weight factors describe the importance of the design parameter and the minimal required torque, and these values are difficult to determine.

An example is the range of motion, defined by the maximum angle the fingers, ϕ_{max} and the initial angle, ϕ_{min} . A large range will probably lead to non optimal results with respect to the minimal torque, in comparison to a smaller range of motion.

Another important design parameter is the width of the concept, l_w , and is measured as the distance between the left and the right finger. Because a static model is used and gravity is neglected the results are scalable, therefore the width of the gripper is used as a reference parameter with a value of 0.10 m. This value is chosen because it is easily scalable and will result in a gripper with an appropriate scale. The position of the middle finger is determined by the distance from the left finger, l_x , and is given a value of 0.05 m. Thereby placing it in the middle of the two other fingers. The depth of the gripper, l_d , is defined as the distance between the two pairs of fingers. And the height of the middle finger, l_z , is defined to be relative to the vertical position of the finger on its left.

Note that the kinematic analysis as described in section III-A provides two solutions for each pyramid, namely one on each side of the base plane. In total this results in four possible configurations from a kinematic point of view. Whether the apex is on the outside or inside of the gripper determines whether the actuator is pulling or pushing the fingers, assuming that the actuator is elongating in both situations.

B. Results

For the cases where the apex of the pyramids lay inside the gripper there were no solutions found where the resulting minimal torques is obtained for the entire workspace. Therefore from all the results in this section describe the configuration where the apexes are outside the gripper. The cause is that the direction in which the linkages are pushing on the finger is almost parallel to the finger itself. This leads to torques in the wrong direction when the angle of the finger moves past the angle of the linkage. This means that the configuration does not satisfy the criteria for the entire workspace.

Figure 5 shows the resulting torques for the configuration where both the apexes are on the outside of the actuator, for each of the design parameters and the height of the finger in the middle. Figure 5(a) shows that the minimal torque decreases as the range of motion of the fingers increases. When the range is about 78 degrees, then the minimal torque becomes zero. For larger ranges of motion there exist no dimensions for which the concept satisfies criteria for the entire workspace. Also note that the average torque, which is about is also decreasing as the range of motion increases, but much slower.

Table I

THIS TABLE CONTAINS THE OPTIMAL DIMENSIONS FOR THE CONCEPT WITH SIX FINGERS AND A LINEAR ACTUATOR. THESE DIMENSIONS ENSURE THAT THE MINIMAL TORQUE ON THE FINGERS IS 0.077 NM FOR ENTIRE WORKSPACE WITH AN ACTUATION FORCE OF 10 N. NOTE THAT THE DIMENSIONS ARE SCALABLE AND THAT THE MINIMUM OUTPUT TORQUE SCALES ACCORDINGLY.

Parameter	Value	m
l_1, l_3, l_4, l_6	0.066	m
l_2, l_5	0.060	m
$l_{f,1}, l_{f,3}, l_{f,4}, l_{f,6}$	0.033	m
$l_{f,3}, l_{f,5}$	0.030	m
l_w	0.100	m
l_x	0.050	m
l_d	0 - 0.150	m
l_z	-0.040	m
ϕ_{min}	0	°
ϕ_{max}	50	°

For further results a range of motion of 50 degrees was chosen. Because this range of motion is considered to be sufficient for actuating underactuated fingers with two phalanges [1], while providing a sufficient minimal torque.

The position of the middle finger is placed initially in the middle of both outer fingers, resulting in a symmetric configuration. In figure 5(b) the corresponding value for l_x is 0.05 m. By moving the middle finger to the finger on the left, the configuration becomes asymmetric and the minimal torque decreases. On the other hand the average and maximum torques increase.

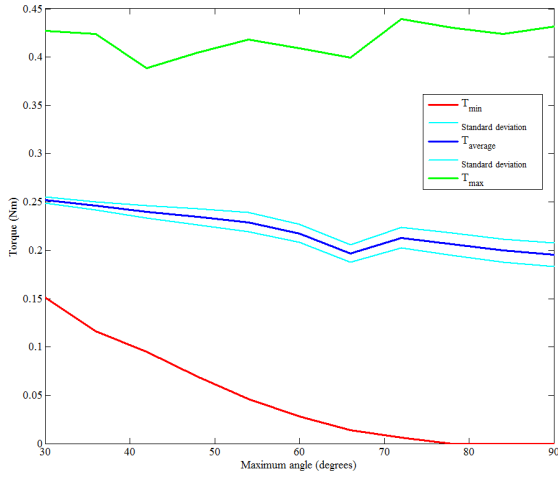
Figure 5(c) depicts the influence of the depth of the gripper, l_d . The minimal torque does not vary for different values of the depth. This also greatly holds for the average torque. The maximum torque varies only slightly and is largest when the depth is smallest.

Finally figure 5(d) shows the influence of the height of the middle finger. The height is indicated as a negative value, because the joint of the middle finger is positioned lower than the outer fingers. Note that the minimal torque increases when the vertical distance increases. Based on these results a minimum of -0.040 m is taken as the minimal height of the middle finger.

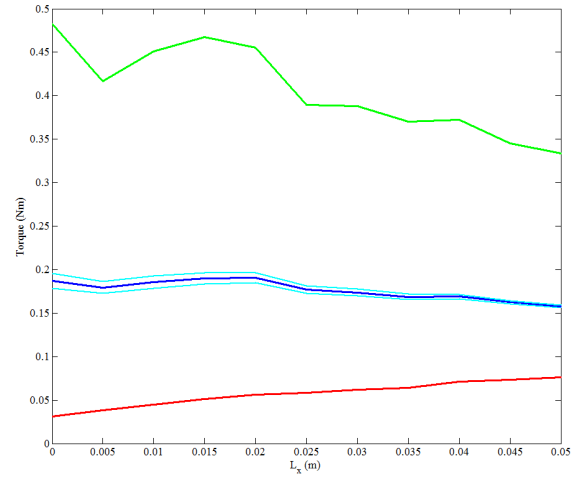
The optimal results for the middle finger, when it is positioned in the middle of both outer fingers and with the minimal height, is given in table I. Increasing the height of the finger will result in a larger minimal torque, but this might not be possible due to design constraints.

C. Conclusion

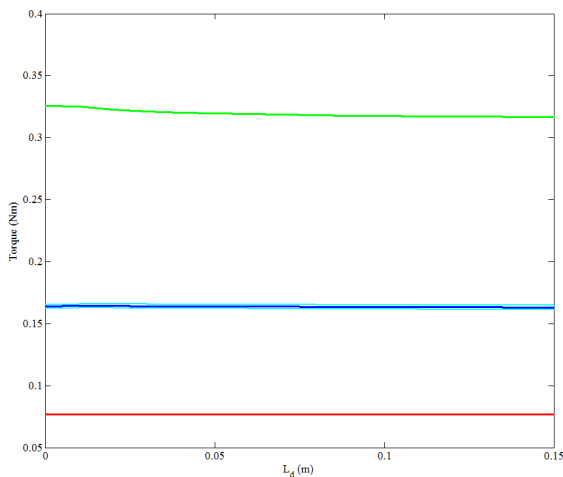
The overall conclusion of the torque analysis for the concept with six fingers and a linear actuator is that the larger the



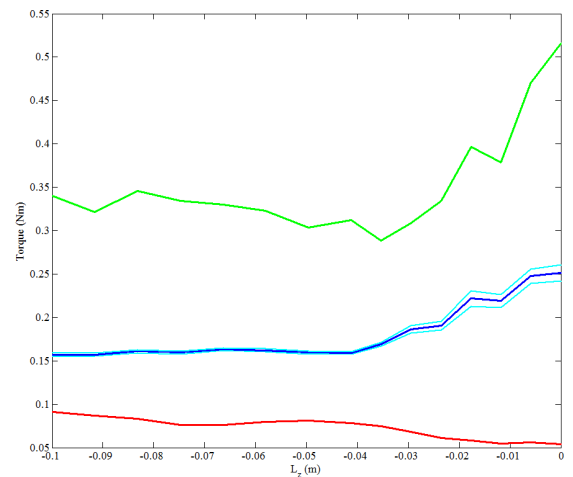
(a) Output torques as a function of the maximum angle, ϕ_{max} .



(b) Output torques as a function of the position of the middle finger, l_x .



(c) Output torques as a function of the depth of the gripper, l_d .



(d) Output torques as a function of the height of the middle finger, l_z .

Figure 5. The influence of the design parameters on the torques of the fingers. Each figure displays the minimal torque, the maximum torque and the average torque of all the fingers. Note that the figures display values for the entire workspace. This means that the average torque is the average for the entire workspace and the minimum and maximum torque is respectively the smallest or largest torque found for one configuration within the workspace.

base of the pyramids the larger the minimal torque becomes. This means that by placing the fingers further apart and on the yz -plane gives better performance. This is caused by the fact that the positions of the apexes of the pyramids displace less when the angles of the fingers change. Assume that the lengths of the fingers stay constant, then each point which spans the base of the pyramid can only be displaced with the same displacement. From here it is obvious that when these points are spaced further apart, that the change of orientation of the base will decrease.

When the pair of fingers are positioned further apart, i.e. increasing the depth of the gripper, l_d . Then the change of the orientation of the actuator becomes smaller, nevertheless according to the results this effect is too small to be noticed.

For a minimal height for the middle finger of -0.040 m and a range of motion of 50 degrees, the resulting minimal torque has a magnitude of 0.077 Nm. The average torque on the fingers is 0.16 Nm, while the actuation force is 10 N. The corresponding optimal dimensions are given in table I.

V. INFLUENCE OF GRAVITY

Section IV showed that it is possible to find a set of dimensions for the concept, such that the output torques comply with the criteria. These dimensions provided a minimum torque of about 0.077 Nm. In this section the influence of the gravity on the concept is investigated. This is essential, because due to the nature of the concept, there does not exist a construction that carries the weight of the actuator. This means that the weight of the actuator is transferred to the output torques of the fingers.

A. Method

Due to the influence of the gravity the gripper will behave different when it is tilted and/or accelerated. To simulate these effects the method as described in section IV-A is extended. More precisely equation IV.1 is extended with one term, see equation V.1. The term contains the gravity and can be set in any orientation relative to the gripper. For this method it is assumed that the center of mass of the actuator lies in the middle, which implies that the gravitational force is distributed equally between both sides.

$$F_{l_1} \hat{\mathbf{v}}_1 + F_{l_2} \hat{\mathbf{v}}_2 + F_{l_3} \hat{\mathbf{v}}_3 - F_{act} \frac{\mathbf{x}_1 - \mathbf{x}_2}{\|\mathbf{x}_1 - \mathbf{x}_2\|} - \frac{\mathbf{F}_g}{2} = \mathbf{0} \quad (\text{V.1})$$

When assessing the influence of the gravity on the output torques, it is essential to make a distinction between the closing motion and the opening motion of the gripper. This is because the direction of the actuation force positive for the closing motion and negative for the opening motion. It is therefore inevitable that the actuation force is at least partially cancelled out by the gravity in one of the motions, while it is strengthened in the other.

The first step is to determine whether the optimal dimensions of the optimization without gravity, see table I, will function in the upright position despite the gravity. Therefore the mass is increased for both the closing and the opening motion, in order

to investigate what the minimal torque is for the corresponding gravitational force.

After the influence of the gravity on the original system is known, it becomes possible to determine whether the minimal torques can be improved by optimizing the dimensions for the case with gravity. The optimization function, IV.4, first assesses the performance of the closing and opening motion independently. After which both motions are assessed simultaneously.

Finally the performance of the optimal dimensions is investigated for the cases where the gripper is rotated with respect to the gravity. In the model the gravity vector is rotated relative to the gripper.

B. Results

Figure 6 shows the influence of a gravitational force on the minimal torques on the fingers for both the closing and opening motions. When assessing the influence for the dimensions, as found in section IV, it can be seen that for the closing motion the minimal torque is increasing until approximately 10 N, after which it is decreasing rapidly and can no longer provide sufficient torque when the gravitational force is larger than 19.5 N. For the opening motion the minimal torque starts decreasing and it can no longer provide sufficient torque when the gravitational force becomes larger than 29 N.

When optimizing the dimensions for the gravitational force results in different curves. For the closing motion the resulting minimal torque is slightly larger for the forces and continues climbing longer until a gravitational force of approximately 21 N. After which the torque gradually decreases.

Optimal dimensions for the opening motion also increase the minimal torque. An additional effect is the increase of the maximum gravitational force the system can handle to 32 N.

The optimization of both motions shows lower minimal torques than in the cases where the torques for one of the

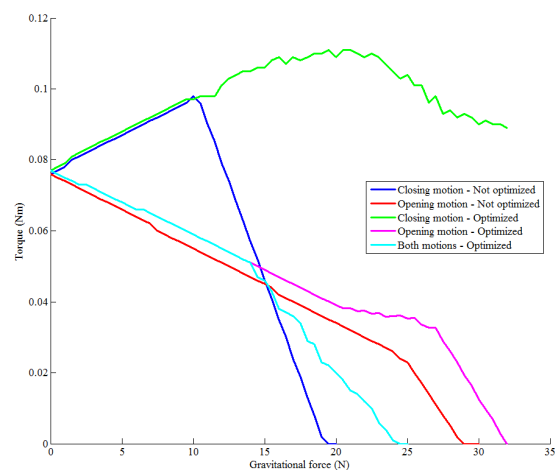
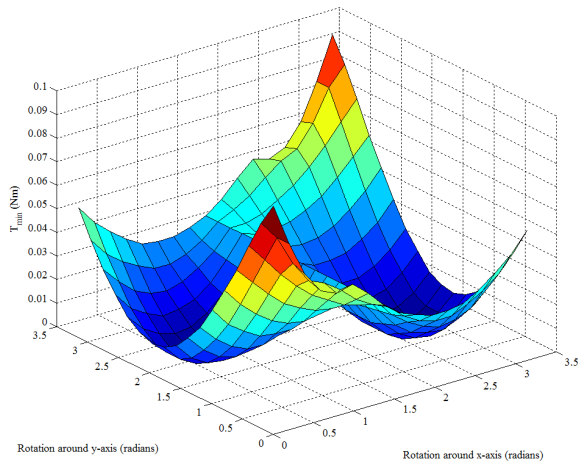
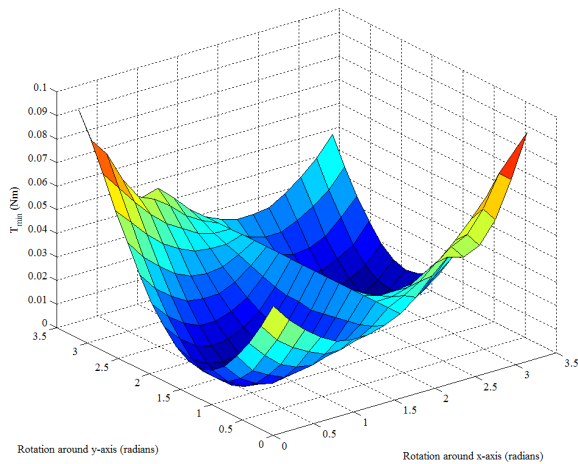


Figure 6. The influence of gravity on the minimal output torques of both the closing and the opening motion is displayed. The figure also displays the resulting minimal torques when the dimensions are optimized for the closing and opening motions, as well as the optimization when both motions are combined.



(a) Closing motion.



(b) Opening motion.

Figure 7. The influence of the maximum gravitational force, of 10.6N, on the minimal output torques of both the closing and the opening motion are displayed in figures 7(a) and 7(b), respectively. The figures display one quadrant of the possible angles of the gravity with respect to the actuator, because the results can be mirrored in the x -axis and y -axis.

motions was optimized. In the lower weight spectrum the opening motion is the limiting factor, though at a certain point the closing motion becomes the limiting factor. In this case the closing motion becomes dominant at a gravitational force of approximately 15 N.

Investigating the effect of a rotated gripper with respect to the gravity revealed a significant influence on the minimal torques, as displayed in figure 7. The maximum gravitational force for which the minimum torques stay above 0 Nm is 10.6 N. These results were obtained with dimensions which proved to be equal to the dimensions found in section IV, when rounded to millimeters. These dimensions are listed in table I.

C. Conclusion

The investigation on the influence of the gravity on the conceptual design shows that it is possible to design a working

floating actuated gripper which can perform under these circumstances. More specifically the results show that it is possible to obtain a torque in the right direction on each finger as long as the ratio between the actuation force and the gravitational force too low. Overall the gravitational force has to be at lower than 1.06 times the actuation force. In this section the calculations were performed with an actuation force of 10 N, which means that the weight of the actuator and linkages combined must be lower than 1.08 kg.

Additionally the investigation for optimizing the dimensions to reduce the effects of gravity for either the closing or opening motion showed that there were conflicting demands on the dimensions. When optimizing the closing motion, for the upright position, the positive effects of the gravity can be utilized with improvements on the minimal torques. Unfortunately these dimensions reduce the performance of the opening motion.

VI. EXPERIMENTS

In this section a prototype of the concept with six fingers and a linear actuator is introduced. The performance of the prototype is determined by performing two experiments. The first experiment will focus on the ability to apply torques for the entire required workspace. The second experiment will investigate the applicability of the gripper in grasp operations.

A. Prototype

The prototype is build up around a linear pneumatic actuator and is depicted in figure 9. The actuator is selected on minimizing both the weight and the dimensions, while maintaining a sufficient stroke and output force. To fit the actuator properly the optimal dimensions found in both section IV and V were scaled by a factor of 0.8. The resulting dimensions are given in table II and correspond with a minimal output torque of 0.062 Nm for each finger. To ensure that the prototype works according to the concept a large number of revolute joints is

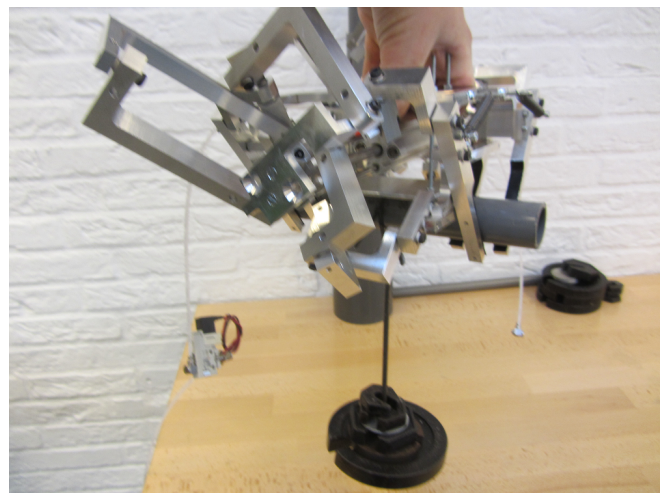
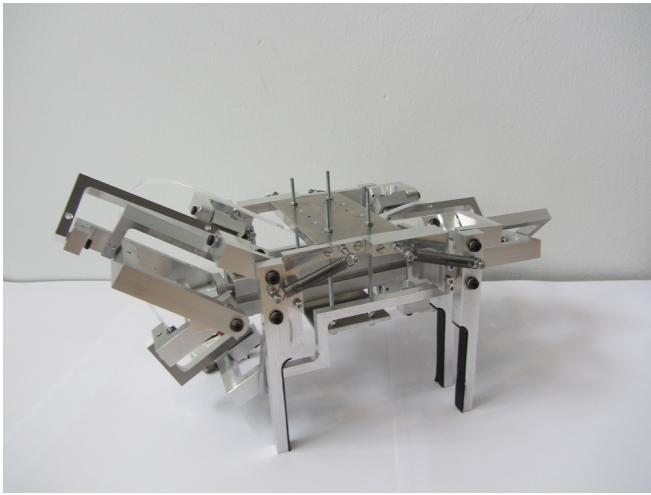
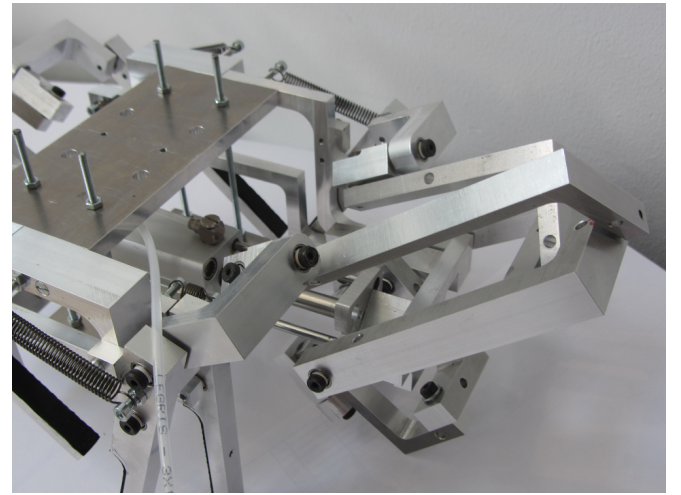


Figure 8. The test setup for the grasp experiment. The prototype grasps cylindrical pvc-pipes with varying diameters. The weight hanging from the pipe is gradually increased until the prototype gripper can no longer hold the pipe.



(a) Side view



(b) Detailed view of the linkages

Figure 9. The prototype of an underactuated gripper with a floating differential actuator. The contact area's of the six fingers can be recognized by the black surface and the revolute joints can be recognized by the black bolts. The linear actuator is positioned in the middle of the gripper. And the linkages in figure 9(b) rotate around the same point of the actuator.

Table II

THIS TABLE CONTAINS THE DIMENSIONS FOR THE PROTOTYPE. THESE DIMENSIONS ENSURE THAT THE MINIMAL TORQUE ON THE FINGERS IS 0.062 NM FOR ENTIRE WORKSPACE WITH AN ACTUATION FORCE OF 10 N.

Parameter	Value	
l_1, l_3, l_4, l_6	0.053	m
l_2, l_5	0.048	m
$l_{f,1}, l_{f,3}, l_{f,4}, l_{f,6}$	0.026	m
$l_{f,3}, l_{f,5}$	0.024	m
l_w	0.080	m
l_x	0.040	m
l_d	0.130	m
l_z	-0.032	m
ϕ_{min}	0	°
ϕ_{max}	50	°

needed, in total 42. To reduce friction in the system as much as possible all joints were fitted with ball-bearings.

An essential part of the concept with six fingers is that both the housing as the axle of the actuator has to be connected with three linkages at the same position. Therefore the prototype had to have three spherical joints with the center of rotation on exactly the same position. The solution to this problem is to split each spherical joint in three revolute joints and position them such that each element could move around another, similar to a planetary system. Note that gimbal lock cannot occur in the case of the prototype, because the rotations are limited due to the closed loop nature of the concept.

Due to the size of the actuator it is necessary to position the middle fingers to the side of the prototype. Otherwise the actuator and these fingers would block each other's motion. As a result the middle fingers are not in the ideal position, which would be in the middle and opposite of each other.

Because the depth of the palm is larger than zero a parallelogram is needed to transfer the torque of the middle finger to the other side of the prototype. Otherwise the finger will rotate in the wrong direction.

B. Workspace Experiment

The goal of the workspace experiment is to determine whether each finger of the prototype is opening and closing for any configuration within the entire workspace. Therefore the motions of several sets of fingers are constrained and the resulting motions of the remaining fingers are observed. This is repeated for various orientations of the prototype. When the actuator is extending the fingers have to make a closing motion and when the actuator is contracting the fingers must return towards the open position.

C. Grasp Experiment

The grasp experiment is designed to investigate the applicability of the prototype for real world applications. For this test the prototype is going to grasp cylindrical objects. The cylindrical objects are pvc-pipes with diameters varying from 19 mm up to 110 mm. Each object is grasped with a preset pressure for the linear actuator. For an impression of the setup see figure 8 For each object the following steps are taken to determine the maximum mass the prototype gripper can hold.

- The prototype has to pick up the object from the table and hold it. During the measurement the prototype remains in an upright orientation.
- When a successful grasp is achieved, then the object is manually repositioned in the prototype to ensure that the center of mass is located in the middle.
- Mass is gradually added to the cylindrical object until the prototype is no longer capable of holding the object. Note that the measurements have a resolution of 0.01 kg.
- Repeat the measurements five times.

The minimum pressure for the pneumatic actuator is 1 bar, which is the minimal required pressure to overcome the static friction in the system. The maximum pressure is 3 bar, despite that the actuator has a nominal working pressure of 6 bar. The maximum is set as a precaution to prevent deformations and damage to the prototype.

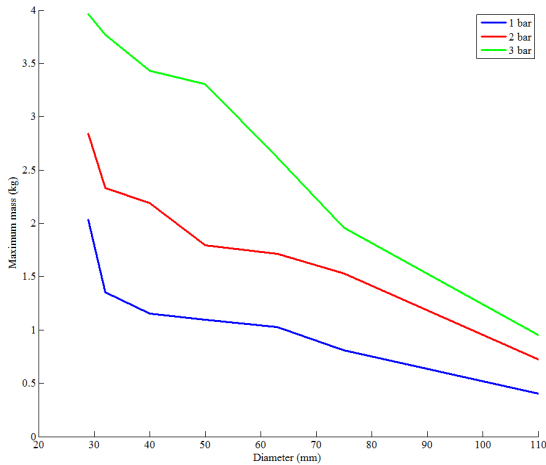


Figure 10. The measured maximum load the prototype is able to hold as a function of the diameter of the cylindrical objects that the prototype grasps. The experiments are performed for three pressures of the pneumatic actuator.

D. Results

The workspace experiment showed that for any configuration the prototype was able to achieve a closing motion for all the fingers. On the other hand, the opening motion was not always achieved, this occurs when the actuator is fully contracted. An additional investigation, where the housing of the actuator was completely constrained, showed that there was significant motion of fingers possible without the actuator extending or contracting. In this case it was observed that the cause is that the chain of joints allowed for sufficient play while requiring relatively little effort.

For the grasp experiment seven objects were used and the results are given in figure 10. The gripper was able to hold up to 0.95 kg for the largest object with a diameter of 110 mm. When the diameter decreases to 19 mm the maximum load increases to 3.96 kg. Especially for the lower pressures it is observed that there is a large increase in the maximum load for the object with smallest diameter.

E. Conclusion

The experiments showed that it was possible to achieve a torque in the desired direction on each of the fingers independent of the configuration of any of the fingers. Except for the situations where the actuator was able to fully contract. Theoretically the prototype should only have one possible configuration for the position of the actuator. Unfortunately changing the position of one of the fingers requires a small elongation of the actuator. In case of the prototype this small difference could also be obtained by play in the entire system. This also allowed the actuator to fully contract without setting all the fingers in the fully open position. Nevertheless the prototype is capable of grasping objects with varying sizes and weights.

The smaller the diameter of the object the larger the mass of the object can be. This is a result of the dependency on the friction to hold objects with larger diameters. For the smaller

object the fingers can close further, which directly increase the vertical component of the force acting on the object.

VII. DISCUSSION

In this report an actuation mechanism for an underactuated gripper is designed for actuating as many fingers as possible by means of an underactuated differential actuator. During this investigation simplifications were made and issues arose. These will be discussed in this section.

A. Grasp Optimization

For the analytical methods in sections III, IV and V the investigation was limited to the output torques of the actuation mechanism. The choice not to optimize grasp performance directly is based on the dependency of the outcome on the design of the fingers. If the grasp performance would be optimized for example for a design with two underactuated phalanges per finger, then the required torques should match the desired torques of the fingers. This requires a different cost function for the optimization, which could lead to other optimal dimensions for the actuation mechanism. Note that a design with two phalanges can reduce the dependency of friction for the objects with a larger diameter, by creating an enveloped grasp.

B. Effect Of Play In The Prototype

During the first tests of the prototype, it became clear that fingers could move independently from the elongation or shortening of the actuator. According to the theory and the applied model this should not be possible. After multiple tests where parts of the prototype were constrained, it became clear that the amount of play in the system allowed for these non-actuated motions. These motions required even in the model very small variations of the length of the actuator. Due to the large number of joints, of which most are also applied in series, these small variations were relatively easy provided by the play. As a result the actuator can fully contract without fully opening all of the fingers. To ensure that the fingers are always capable of returning to the fully opened position, springs were added. Once a grasp is achieved the prototype is locked in the desired position and then the play is no longer noticeable.

C. Prototype Complexity

The main reason to implement underactuated mechanisms in grippers is to reduce the complexity of the design. The prototype, as presented in this report, cannot be classified as a simple mechanism, while the concept could allow for less complex designs. One option is to replace all the linkages and revolute joints by linkages with compliant joints, significantly reducing the number of parts. When the opening motion is made completely passive then the linkages can be replaced by cables, simplifying the design even further.

The prototype cannot be considered to be a simple design compared to other underactuated grippers [3]. As a result the prototype, in its current state, will probably not be an economically viable alternative to the underactuated grippers

that are currently used. Nevertheless it shows that it is possible to actuate six fingers without the need for traditional differential mechanisms. It therefore might be possible that the simplification, by using cables for the linkages, can result in a design which is economically viable.

D. Future Work

In order to prevent non-actuated motions in future prototypes from happening, it is advised to ensure that larger elongations of the actuator are necessary, because it is very difficult to remove the play in the components that build the prototype.

An alternative could be to design a system that where the degrees of freedom are provided by means of compliant joints or cables, thereby reducing the weight of the system, complexity of the system and ultimately the cost of the system.

VIII. CONCLUSION

The primary goal of this investigation was to find the maximum number of output that could be actuated by a differential actuator. Section III showed that it was not possible to find a system that could actuate the theoretical maximum of seven outputs for a relevant workspace. The main cause appears to be the kinematic restraints introduced by dependencies between the orientation of the actuator and the distance constraints of the actuator with respect to the fingers. For the case with six fingers the orientation of the actuator becomes less prominent, thereby allowing independent motions for the required workspace.

This report presents in section VI-A, a working design for an underactuated gripper with six fingers and a differential linear actuator. The differential nature of the actuator allowed it to distribute the actuation force over six outputs independently while allowing for independent motions of the fingers.

REFERENCES

- [1] C. Meijneke, G. A. Kragten, and M. Wisse, "Design and Performance Assessment of an Underactuated Hand for Industrial Applications," *Mechanical Sciences*, vol. 2, no. 1, pp. 9–15, 2011.
- [2] A. Gerritse, *Design of a Vine Tomato Gripper*. Bachelor thesis, Hogeschool Utrecht, 2011.
- [3] L. Birglen, T. Laliberté, and C. M. Gosselin, *Underactuated Robotic Hands*, vol. 40. Springer Berlin Heidelberg, 2008.
- [4] W. Townsend, "The BarrettHand Grasper: Programmably Flexible PartHandling and Assembly," *Industrial Robot: An International Journal*, vol. 27, no. 3, pp. 181–188, 2000.
- [5] J. Pons, E. Rocon, R. Ceres, D. Reynaerts, B. Saro, S. Levin, and W. Van Moorleghem, "The MANUS-Hand - Dextrous Robotics Upper Limb Prosthesis: Mechanical and Manipulation Aspects," *Autonomous Robots*, vol. 16, pp. 143–163, 2004.
- [6] S. Krut, "A Force-Isotropic Underactuated Finger," in *Robotics and Automation, IEEE International Conference on*, vol. 2, pp. 2314–2319, IEEE, 2005.
- [7] M. Kaneko, M. Higashimori, A. Namiki, and M. Ishikawa, "The 100G Capturing Robot: Too Fast to See," *Robotics Research. The Eleventh International Symposium*, vol. 15, pp. 517–526, 2005.
- [8] S. Hirose and Y. Umetani, "The Development of Soft Gripper for the Versatile Robot Hand," *Mechanism and Machine Theory*, vol. 13, no. 1, pp. 351–359, 1978.
- [9] F. Lotti, P. Tiezzi, G. Vassura, L. Biagiotti, and C. Melchiorri, "UBH 3 : an Anthropomorphic Hand with Simplified Endo-Skeletal Structure and Soft Continuous Fingerpads," in *Robotics and Automation, IEEE International Conference on*, no. April, (New Orleans), pp. 4736–4741, 2004.
- [10] S. Yao, M. Ceccarelli, Q. Zhan, G. Carbone, and Z. Lu, "Analysis and design of a modular underactuated mechanism for robotic fingers," *Proceedings of the Institution of Mechanical Engineers, Part C: Journal of Mechanical Engineering Science*, vol. 226, no. 1, pp. 242–256, 2011.
- [11] A. M. Dollar and R. D. Howe, "The SDM Hand as a Prosthetic Terminal Device: A Feasibility Study," in *Rehabilitation Robotics, IEEE International Conference on*, no. June, (Noordwijk), pp. 1–6, 2007.
- [12] C. Gosselin, F. Pelletier, and T. Lalibert, "An Anthropomorphic Underactuated Robotic Hand with 15 Dofs and a Single Actuator," in *Robotics and Automation, IEEE International Conference on*, (Pasadena, California), pp. 749–754, 2008.
- [13] N. Fukaya, S. Toyama, T. Asfour, and R. Dillmann, "Design of the TUAT / Karlsruhe Humanoid Hand," in *Proceedings of the 2000 IEEE/RSJ International Conference on Intelligent Robots and Systems*, pp. 1754–1759, 2000.
- [14] T. Laliberté, M. Baril, F. Guay, and C. Gosselin, "Towards the Design of a Prosthetic Underactuated Hand," *Mechanical Sciences*, vol. 1, pp. 19–26, Dec. 2010.
- [15] M. Myrand, *Simulation Dynamique d'une Main Robotique Sous-Actionnée*. Phd thesis, Université Laval, 2004.
- [16] O. Sigmund, "On the Design of Compliant Mechanisms Using Topology Optimization," *Mechanics of Structures and Machines: An International Journal*, vol. 25, no. 4, pp. 493–524, 1997.
- [17] M. Doria and L. Birglen, "Design of an Underactuated Compliant Gripper for Surgery Using Nitinol," *Journal of Medical Devices*, vol. 3, no. 1, p. 011007, 2009.
- [18] T. Laliberté and C. M. Gosselin, "Actuation System for Highly Underactuated Gripping Mechanism," United States Patent no. 6,505,870, 2003.
- [19] S. Nasser, D. Rincon, and M. Rodriguez, "Design of an Anthropomorphic Underactuated Hand Prosthesis with Passive-Adaptive Grasping Capabilities," in *Florida Conference on Recent Advances in Robotics*, (Miami, Florida), pp. 1–7, 2006.
- [20] V. Bégo, S. Krut, E. Dombre, C. Durand, and F. Pierrot, "Mechanical Design of a New Pneumatically Driven Underactuated Hand," in *IEEE International Conference on Robotics and Automation*, pp. 927–933, 2007.
- [21] B. Massa, S. Roccella, M. Carrozza, and P. Dario, "Design and development of an underactuated prosthetic hand," in *Proceedings of the 2002 IEEE International Conference on Robotics and Automation*, vol. 4, pp. 3374–3379, IEEE, 2002.
- [22] V.-D. Nguyen, "Constructing Force-Closure Grasps," *The International Journal of Robotics Research*, vol. 7, no. 3, pp. 3–16, 1988.
- [23] J. Z. Zheng, S. De La Rosa, and A. M. Dollar, "An investigation of grasp type and frequency in daily household and machine shop tasks," *2011 IEEE International Conference on Robotics and Automation*, pp. 4169–4175, 2011.
- [24] Q. Jiang, *Singularity-Free Workspace Analysis and Geometric Optimization of Parallel Mechanisms*. Phd thesis, Université Laval, 2008.

APPENDIX A
KINEMATIC ANALYSIS FOR ROTARY CONCEPTS

In this appendix the details of the kinematic analysis for the concepts driven by a rotary actuator are described. The kinematic analysis investigates whether the constraint equations describing the system can be solved for each set of design parameters and input parameters.

A. Derivation of the Constraint Equations

The first step in the kinematic analysis is to derive the constraint equations which are used to determine the position and the orientation of the actuator. The input values are the angles of the fingers with respect to the origin. In short this means that the model is build from the ground up, first the position of the joint between the linkage and the finger, denoted by \mathbf{f}_j , are to be determined. Equation A.1 describes a rotation around the global x-axis and gives the relation between the length of the finger, $l_{f,j}$, the center of rotation, $\mathbf{x}_{f,j}$, and the angle ϕ_j . Note that both $l_{f,j}$ and $\mathbf{x}_{f,j}$ are design parameters and ϕ_j is the input parameter.

$$\mathbf{f}_j = \mathbf{R}_x(\phi_j)l_{f,j} + \mathbf{x}_{f,j} \quad (\text{A.1})$$

Here the rotation matrix around the x-axis $\mathbf{R}_x(\phi)$ is given by equation A.2.

$$\mathbf{R}_x(\phi) = \begin{pmatrix} 1 & 0 & 0 \\ 0 & \cos \phi & -\sin \phi \\ 0 & \sin \phi & \cos \phi \end{pmatrix} \quad (\text{A.2})$$

The degrees of freedom of the actuator are given by A.3, A.4 and A.5. Here \mathbf{x} is the global position of the center of rotation of the rotor with the stator. And \mathbf{q} is the orientation of the stator described by a quaternion. The angle between the stator and the rotor is ϕ_{act} .

$$\mathbf{x} = \begin{pmatrix} x \\ y \\ z \end{pmatrix} \quad (\text{A.3})$$

$$\mathbf{q} = \begin{pmatrix} q_0 \\ q_1 \\ q_2 \\ q_3 \end{pmatrix} \quad (\text{A.4})$$

$$\phi_{act} \quad (\text{A.5})$$

For each linkage connected to the stator of the actuator the corresponding constraint equation is given by equation A.6. Here the length of the linkage is denoted by l_j . The position of the connection between the actuator and the linkage is denoted by \mathbf{p}_j , where this position is relative to the center of rotation of the actuator, \mathbf{x} .

$$C_{s,j} = \|\mathbf{R}(\mathbf{q})\mathbf{p}_j + \mathbf{x} - \mathbf{f}_j\| - l_j \quad (\text{A.6})$$

In case the linkage is connected to the rotor of the actuator, then the constraint equation is given by equation A.7.

$$C_{r,j} = \|\mathbf{R}(\mathbf{q})\mathbf{R}_x(\phi_{act})\mathbf{p}_j + \mathbf{x} - \mathbf{f}_j\| - l_j \quad (\text{A.7})$$

Here the rotation matrix of a quaternion is calculated according to equation A.8 and the rotation of the rotor is determined according to equation A.2.

$$\mathbf{R}(\mathbf{q}) = \begin{pmatrix} q_0^2 + q_1^2 + q_2^2 + q_3^2 & 2(q_1q_2 - q_0q_3) & 2(q_0q_2 + q_1q_3) \\ 2(q_1q_2 + q_0q_3) & q_0^2 + q_1^2 + q_2^2 + q_3^2 & 2(q_2q_3 - q_0q_1) \\ 2(q_1q_3 - q_0q_2) & 2(q_0q_1 + q_2q_3) & q_0^2 + q_1^2 + q_2^2 + q_3^2 \end{pmatrix} \quad (\text{A.8})$$

Note that it is required that a quaternion is always represented by a unit-vector, therefore the norm of the quaternion has to be equal to 1, resulting in an additional constraint equation A.9.

$$C_q = \|\mathbf{q}\| - 1 \quad (\text{A.9})$$

The complete set of constraint equations is given by A.10 for n fingers. For each finger one has to define whether it is connected to the stator or the rotor of the actuator.

$$\mathbf{C} = \begin{pmatrix} C_{s,1} & or & C_{r,1} \\ & \vdots & \\ C_{s,n} & or & C_{r,n} \\ & C_q & \end{pmatrix} \quad (\text{A.10})$$

B. Evaluation of the Constraint Equations

The second step in the kinematic analysis is to evaluate whether a solution can be found for the degrees of freedom of the actuator. The design parameters are provided by the optimization algorithm, which is described in section A-C. Therefore the design parameters are considered to be known for this section. For the evaluation of the constraint equations Newton's iteration method is used. The iteration method tries to minimize the error, which in this case is equal to the result of the constraint equations, A.11.

$$\mathbf{e} = \mathbf{C} \quad (\text{A.11})$$

Each iteration step the degrees of freedom, Q , are modified. Either until a solution is found where the error is smaller than a preset tolerance, in this case $1e-10$. Or until the maximum number of iterations is reached, meaning that a solution is not found. The degrees of freedom are modified according to equation A.12

$$\mathbf{Q} = \mathbf{Q} - \mathbf{J}^+ \mathbf{e} \quad (\text{A.12})$$

Here \mathbf{J}^+ is the Moore-Penrose pseudoinverse of the jacobian matrix of the constraint equation, \mathbf{J} . The pseudoinverse is given by equation A.13.

$$\mathbf{J}^+ = \mathbf{J}^T (\mathbf{J}^T \mathbf{J})^{-1} \quad (\text{A.13})$$

Note that the jacobian \mathbf{J} is determined by equation A.14 and contains all the partial derivatives of the constraint equations, \mathbf{C} , as functions of the degrees of freedom, \mathbf{Q} .

$$\mathbf{J} = \frac{d\mathbf{C}}{d\mathbf{Q}} \quad (\text{A.14})$$

The evaluation function returns a boolean, which is *true* when a solution is found and *false* when it is not possible to find a solution which satisfies the constraint equations.

C. Optimization Method

The final step in the kinematic analysis is to find a set of design parameters for which the workspace of the concept is maximized. The workspace is defined by the possible combinations of angles of the fingers, ϕ_j . Due to the complexity of the system an optimization method is needed to determine the design parameters for which the workspace is largest. The optimization method used is the *fminsearch*-function as implemented in *Matlab*. For each combination of input parameters the evaluation, as described in section A-B, is used and when a kinematic solution is possible then the cost value, q_{cost} , is decreased by 1. After each discrete position in the desired workspace is evaluated the cost value is normalized, such that the cost value always lies in the range $[0,-1]$, where -1 means that the entire required workspace can be reached with the optimal design parameters.

D. Parameters

For the optimization method a large number of design parameters are available. The most influential parameter to vary is which fingers are connected to the rotor. In this evaluation it was chosen to divide the fingers equally over the stator and the rotor. In case of the rotary concept with seven fingers, this implies that the stator is connected to four linkages and the rotor has three linkages connected to itself. The reasoning behind this is that each part of the actuator is most likely to be capable of providing independent motion for the fingers when the number of connections is minimal for each part.

To minimize the amount of variations of the design parameters in the first phase of the optimization constant parameters for the centers of rotations of the fingers, $\mathbf{x}_{f,j}$, are defined. Here the fingers were again divided in two pairs which were positioned opposite of each other. In the case of the concept with seven fingers, one side has four fingers. The distance between the outer fingers is set as 0.1 m, the distance between the fingers is 0.05 m for the side with three fingers and 0.034 m for the side with four fingers. The width of the palm, e.g. the distance between the pairs of fingers, is 0.08 m. Also the range of the angle for each finger, ϕ_j , are considered constant and set to $[-25, 25]$ degrees. The total range of motion of 50 degrees is similar to the gripper designed by Meijneke et al. [1]. When it appears that the system can handle this range of motion, then it will be increased.

The positions where the linkages are connected to the actuator are denoted by \mathbf{p}_j . These positions will be described by polar coordinates, as given by equation A.15. The value $l_{p,j}$ is the arm of the linkage relative to the axis of rotation of the actuator. The initial angle of the arm is given by $\phi_{p,j}$ and the arm is orientated upwards when this value is 0. The offset parallel to the axis of rotation, $x_{p,j}$ is negative for the rotor and positive for the stator, ensuring that the center of rotation always lies between the rotor and the stator. The lengths can be varied by the optimization method between the interval $[0.010, 0.100]$. This also holds for the lengths of the linkages, l_j .

$$\mathbf{p}_j = \begin{pmatrix} x_{p,j} \\ l_{p,j} \sin \phi_{p,j} \\ l_{p,j} \cos \phi_{p,j} \end{pmatrix} \quad (\text{A.15})$$

APPENDIX B
KINEMATIC AND TORQUE ANALYSIS FOR LINEAR CONCEPTS

In this appendix the details of the kinematic analysis are described. The kinematic analysis investigates whether the constraint equations describing the system can be solved for each set of design parameters and input parameters.

A. Derivation of the Constraint Equations

The first step in the kinematic analysis is to derive the constraint equations which are used to determine the position and the orientation of the actuator. The input values are the angles of the fingers with respect to the origin. In short this means that the model is build from the ground up, first the position of the joint between the linkage and the finger, denoted by \mathbf{f}_j , are to be determined. Equation B.1 describes a rotation around the global x-axis and gives the relation between the length of the finger, $l_{f,j}$, the center of rotation, $\mathbf{x}_{f,j}$, and the angle ϕ_j . Note that both $l_{f,j}$ and $\mathbf{x}_{f,j}$ are design parameters and ϕ_j is the input parameter.

$$\mathbf{f}_j = \mathbf{R}_x(\phi_j)\mathbf{l}_{f,j} + \mathbf{x}_{f,j} \quad (\text{B.1})$$

Here the rotation matrix around the x-axis $\mathbf{R}_x(\phi)$ is given by equation B.2.

$$\mathbf{R}_x(\phi) = \begin{pmatrix} 1 & 0 & 0 \\ 0 & \cos \phi & -\sin \phi \\ 0 & \sin \phi & \cos \phi \end{pmatrix} \quad (\text{B.2})$$

The degrees of freedom of the actuator are given by B.3 and B.4. Here \mathbf{x}_s is the global position of the stator of the actuator and \mathbf{x}_r is the global position of the rod.

$$\mathbf{x}_s = \begin{pmatrix} x_s \\ y_s \\ z_s \end{pmatrix} \quad (\text{B.3})$$

$$\mathbf{x}_r = \begin{pmatrix} x_r \\ y_r \\ z_r \end{pmatrix} \quad (\text{B.4})$$

For the concepts with a linear actuator all the points where the linkage are connected, \mathbf{p}_j , are positioned at the same location for both the stator or the rod. Because a static analysis it is possible to simplify the equations by choosing the reference position each the part to be at the same location as the points where the linkage connect, resulting in B.5 and B.6 for respectively the stator and the rod.

$$\mathbf{x}_s = \mathbf{p}_1 = \mathbf{p}_2 = \mathbf{p}_3 \quad (\text{B.5})$$

$$\mathbf{x}_r = \mathbf{p}_4 = \mathbf{p}_5 = \mathbf{p}_6 \quad (\text{B.6})$$

The resulting situation for both the stator and the rod is depicted in figure 11. The distance between \mathbf{x}_s and \mathbf{x}_r defines what the length of the linear actuator must be for the corresponding configuration. Therefore it is possible to separate the configuration in two constraint problems, one describing the position of the stator and the other of the rod. The resulting constraint equations are then three distance constraints for each pyramid, given by equation B.7.

$$\|\mathbf{x} - \mathbf{f}_1\| - l_1 = 0 \quad (\text{B.7a})$$

$$\|\mathbf{x} - \mathbf{f}_2\| - l_2 = 0 \quad (\text{B.7b})$$

$$\|\mathbf{x} - \mathbf{f}_3\| - l_3 = 0 \quad (\text{B.7c})$$

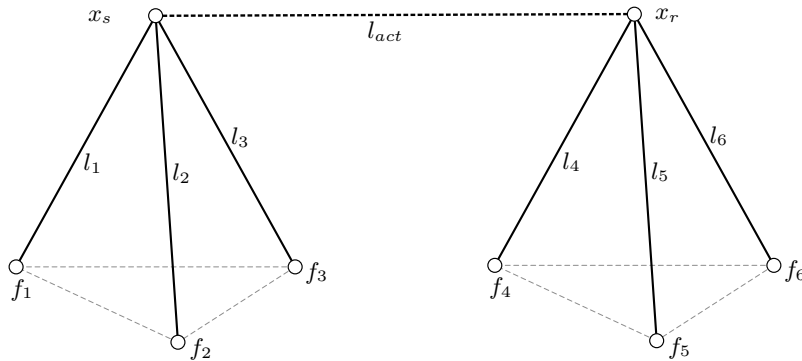


Figure 11. The two triangulation problems for which the apexes x_s and x_r need to be found. The linkages have a length, l_j , which determines the distance between a base point, f_j , and the corresponding apex. The base points are the points where the linkages are connected to the fingers. The distance between the apexes defines what the length of the linear actuator must be for the given configuration. Note that a second solution exists, this solution is the symmetric solution on the other side of the base.

B. Gaussian Elimination

Now the constraint equations are known it is time to determine the values for the positions. In order to do so the constraint equations are first rewritten to equation B.8.

$$(x - x_{f,1})^2 + (y - y_{f,1})^2 + (z - z_{f,1})^2 - l_1^2 = 0 \quad (\text{B.8a})$$

$$(x - x_{f,2})^2 + (y - y_{f,2})^2 + (z - z_{f,2})^2 - l_2^2 = 0 \quad (\text{B.8b})$$

$$(x - x_{f,3})^2 + (y - y_{f,3})^2 + (z - z_{f,3})^2 - l_3^2 = 0 \quad (\text{B.8c})$$

Restructuring the equations such that only terms of x remain on the left side results in B.9.

$$x^2 - 2x_{f,1}x = l_1^2 - (y - y_{f,1})^2 - (z - z_{f,1})^2 - x_{f,1}^2 \quad (\text{B.9a})$$

$$x^2 - 2x_{f,2}x = l_2^2 - (y - y_{f,2})^2 - (z - z_{f,2})^2 - x_{f,2}^2 \quad (\text{B.9b})$$

$$x^2 - 2x_{f,3}x = l_3^2 - (y - y_{f,3})^2 - (z - z_{f,3})^2 - x_{f,3}^2 \quad (\text{B.9c})$$

For the next step the variables y and z are considered to be constant and simplifying the equations result in B.10.

$$x^2 + ax = A(y, z) \quad (\text{B.10a})$$

$$x^2 + bx = B(y, z) \quad (\text{B.10b})$$

$$x^2 + cx = C(y, z) \quad (\text{B.10c})$$

Applying Gaussian row elimination only on the first column only gives the following equations B.11.

$$x^2 + ax = A(y, z) \quad (\text{B.11a})$$

$$bx = B(y, z) - A(y, z) \quad (\text{B.11b})$$

$$x = \frac{C(y, z) - A(y, z)}{c} \quad (\text{B.11c})$$

Substituting equation B.11c in equations B.9a and B.9b and reordering these equations such that only terms of y remain on the left side results in equations B.12. Here only z is considered to be constant and the notation of the equations is simplified.

$$y^2 + dy = D(z) \quad (\text{B.12a})$$

$$y^2 + ey = E(z) \quad (\text{B.12b})$$

Applying Gaussian row elimination gives the following equations B.13.

$$y^2 + dy = D(z) \quad (\text{B.13a})$$

$$y = \frac{E(z) - D(z)}{e} \quad (\text{B.13b})$$

Substituting equations B.13b in equation B.12a and reordering these equations such that only terms of z remain on the left side results in equation B.14.

$$z^2 + fz = F \quad (\text{B.14})$$

The solutions for z are then given by B.15.

$$z = \frac{-f \pm \sqrt{f^2 - 4F}}{2} \quad (\text{B.15})$$

Now the value of z is known it is possible to find the values of y and x by back-substitution. Note that two solutions exist were the solutions are symmetric solution but located on opposite sides of the base of the pyramid. If the solution has an imaginary part then a kinematic solution for the pyramid does not exist. Note that if the discriminant of equation B.15 can become zero for a given configuration, then the back-substitution only returns one solution. In those cases it is better to choose another order in which the Gaussian elimination is performed, for instance z, y, x order instead of the current order of x, y, z .

The final step is selecting the relevant solution for the configuration that one wants to analyze. The only prerequisite is that the solution must always remain at the same side of the base of the pyramid. In other words the solution may not flip to the other side of the base during an analysis.

C. Derivation of the Torques

When a kinematic solution exists then it is possible to determine the torques on the fingers, T_j , applied by the actuation force, F_{act} , of the actuator. Note that for positive values of the actuation force the actuator is extending, otherwise it is contracting. The set of equations B.16a provide three equations from which the magnitudes of the forces by the actuator on the linkages can be determined for the stator. For the rod this is possible with equations B.16b. Note that the gravitational force, \mathbf{F}_g , can be directed in any orientation to simulate different orientations of the gripper in the real world. During this simulation the assumption is made that the center of mass always in the middle of the actuator which means that the gravitational force in equation B.16a is equal to the gravitational force in B.16b.

$$F_{l,1}(\mathbf{x}_{f,1} - \mathbf{x}_s) + F_{l,2}(\mathbf{x}_{f,2} - \mathbf{x}_s) + F_{l,3}(\mathbf{x}_{f,3} - \mathbf{x}_s) = F_{act}(\mathbf{x}_s - \mathbf{x}_r) + \mathbf{F}_g \quad (\text{B.16a})$$

$$F_{l,4}(\mathbf{x}_{f,4} - \mathbf{x}_r) + F_{l,5}(\mathbf{x}_{f,5} - \mathbf{x}_r) + F_{l,6}(\mathbf{x}_{f,6} - \mathbf{x}_r) = F_{act}(\mathbf{x}_r - \mathbf{x}_s) + \mathbf{F}_g \quad (\text{B.16b})$$

The force the linkage is exerting on the finger, $\mathbf{F}_{f,j}$, is given by equation B.17, in vector-form. Here \mathbf{x} is either \mathbf{x}_s or \mathbf{x}_r depending on which of the two the corresponding linkage is connected to.

$$\mathbf{F}_{f,j} = F_{l,j}(\mathbf{x}_{f,j} - \mathbf{x}) \quad (\text{B.17})$$

Because the finger is suspended by a revolute joint the force parallel to the axis, $F_{x,j}$, does not contribute to the torque in the desired direction. The torque exerted on the fingers is given by equation B.18.

$$T_{f,j} = F_{f,j,x}l_{f,j}\sin(\phi_j) - F_{f,j,z}l_{f,j}\cos(\phi_j) \quad (\text{B.18})$$

D. Optimization Method

The final step in the analysis is to find a set of design parameters for which the minimal torque that occurs in the workspace of the concept is maximized. The workspace is defined by the possible combinations of angles of the fingers, ϕ_j . The optimization method used is the *fminsearch*-function as implemented in *Matlab*. For each combination of input parameters the kinematics and the torques are evaluated. When a kinematic solution exists then the signs of the torques on the fingers, T_j , is checked. If all the signs are correct then the magnitude of the torques is checked. Each torque has to have a magnitude larger than a predefined minimal torque, T_{min} . When this is true for all fingers than, the cost value, q_{cost} , is decreased by 1. When all combinations of input parameters are checked, then the cost value is normalized, such that the cost value always lies in the range [0,-1], where -1 means that the entire required workspace can be reached and that the minimal torque T_{min} is guaranteed for each finger. During the first iteration of the optimization the minimal torque is set to 0 Nm. When the optimization returns a cost value of -1, then the minimal torque is increased gradually with a resolution of 0.001 Nm.

E. Parameters

The investigation of the concepts driven by linear actuators is limited to grippers with six fingers, which are divided in two pairs. The pair of fingers are positioned opposite of each other, with a distance w . This distance defines the y-position of the center of rotation of the fingers, $\mathbf{x}_{f,j}$. The fingers positioned on the outside of each group are at a distance of 0.10 m of each other. This value acts as a reference value and is predefined and therefore does not change during the optimization process. All the outer fingers remain on the reference height, meaning this value is 0 m. The height of the finger and the position on the x-axis of the middle finger is optimized. As well as the lengths of the fingers, $l_{f,j}$, which have a minimal value of 0.01 m.

The total interval of the angles of the fingers is 50 degrees, this is similar to gripper designed by Meijneke et al. [1], as is considered sufficient. The initial angle of the fingers is optimized, thereby changing the range of motion of the fingers.

The remaining parameters are the lengths of the linkages connecting the fingers to the actuator. These lengths are most important for the performance of the concept. When these lengths are either too long or too short then it might occur that there does not exist a kinematic solution for the entire workspace. The lengths of the linkages are also optimized.

APPENDIX C TORQUE CURVES OF THE OPTIMAL DESIGN

In this appendix the torque curves of the optimal design are discussed. The torque curves given are those which are most relevant for the performance of the concept.

A. Torque

The motion where all the fingers will close simultaneously will probably occur most when using the prototype. In figure 12 the torque curves for this motion are given. The torque curves all have approximately the same shape. Only the magnitude of the finger in the middle is significantly higher. This is a result of the fact that the middle finger has to compensate the vertical force component of both fingers on the outside. For this common closing motion the optimal design is able to provide at least 0.1 Nm on each finger with an actuation force of 10 N.

The minimal torque found in the workspace occurs in the situation where two fingers on one side of the actuator are in the open position and the other four fingers are in the closed position. Figure 13(a) shows the situation where the fingers in the middle are closing simultaneously. For the set of optimal dimensions the minimal torque is 0.077 Nm.

B. Minimal Actuator Elongation

The experiments with the prototype showed that it was possible to move some fingers completely without extending the actuator. According to the model the actuator always needs to extend to allow the fingers to close. For the optimal design the minimal elongation is 0.015 m. This is for the case where only one finger on the outside is closing, while the other fingers remain open. And is depicted in figure 13(b). Apparently the play in the system is equivalent to an elongation of at least 0.015 m.

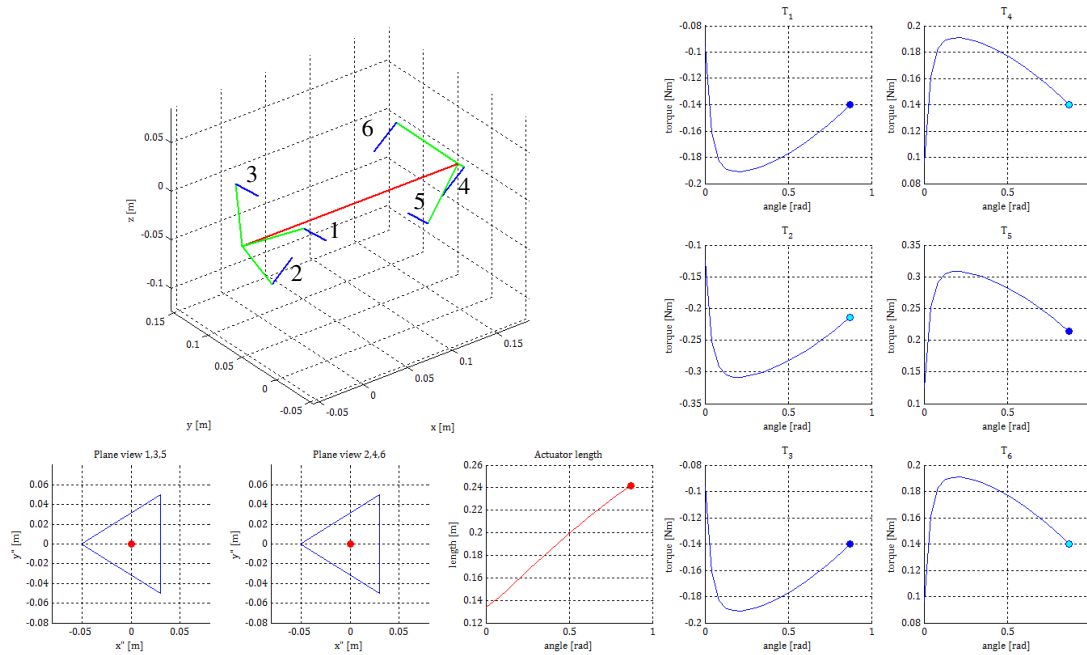
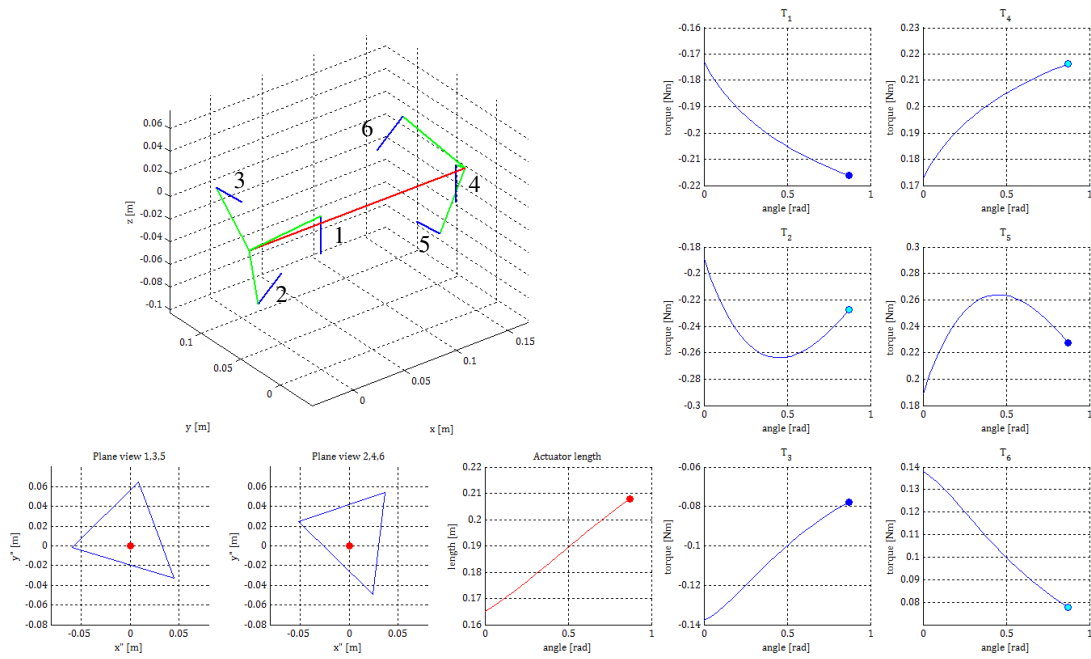
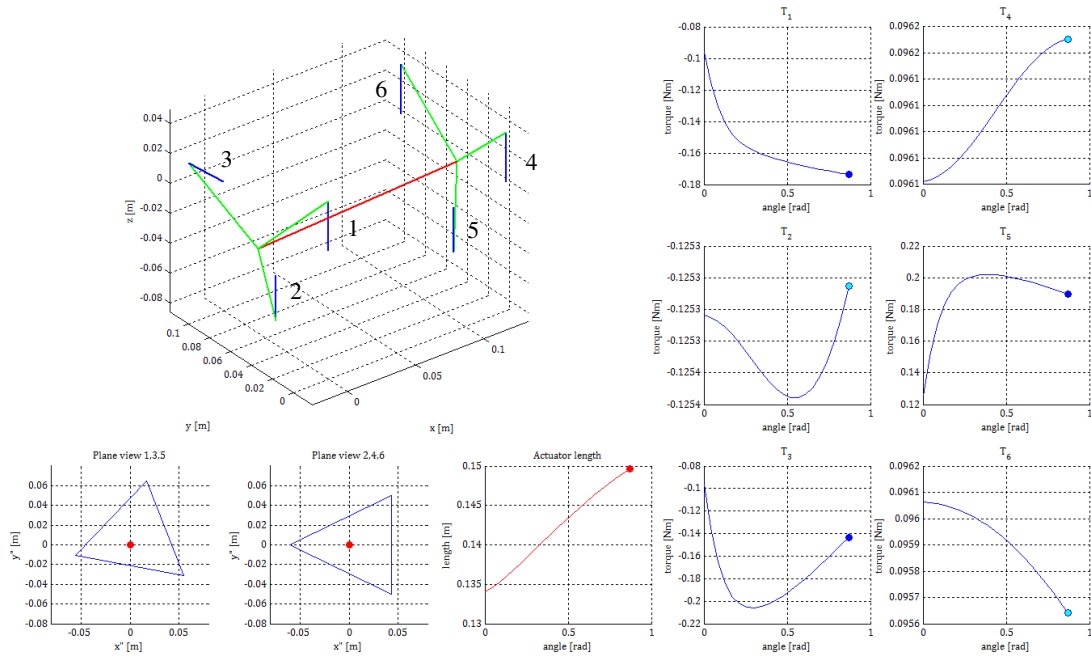


Figure 12. Torque curve of the optimal design for the situation where all fingers close simultaneously. The upper left figure shows the configuration, where the fingers (blue) are numbered. The fingers are connected to the actuator (red) by linkages (green). The six graphs on the right show the torque curves for each of the motions. The graph in the bottom middle shows the length of the actuator. The two remaining graphs on the bottom left show the area in which the intersection of the actuation force with the base plane must remain, otherwise the output torque will change direction.



(a) Torque curves for the motion with lowest torque. Fingers 2 and 5 are closing and fingers 3 and 6 remain closed and fingers 1 and 4 remain open.



(b) Torque curves for the motion with shortest elongation of the actuator. Only finger 3 is closing the other fingers remain in the open position.

Figure 13. Torque curves of the optimal design. The upper left figure shows the configuration, where the fingers (blue) are numbered. The fingers are connected to the actuator (red) by linkages (green). The six graphs on the right show the torque curves for each of the motions. The graph in the bottom middle shows the length of the actuator. The two remaining graphs on the bottom left show the area in which the intersection of the actuation force with the base plane must remain, otherwise the output torque will change direction.

APPENDIX D DETAILS OF THE PROTOTYPE

In this appendix the details of the design of the prototype are discussed. The prototype is designed and manufactured to proof the working principle as proposed in this report. Therefore the design is not optimal in terms of cost-efficiency and weight, but is build robustly to perform the required tests. The prototype is completely made of aluminum and publicly available parts, such as the linear actuator.

A. Actuator

The prototype is driven by a pneumatic linear actuator. The dimensions of the actuator have large implications on the final design of the prototype, because it required a significant amount of space. The stroke of the actuator is the decisive parameter for selection of the right actuator. The most suitable actuator proved to be a compact pneumatic cylinder from the ADNGF-line made by Festo, see figure 14(a). The cylinder is guided, which means that the housing and the shaft cannot rotate relative to each other. The cylinder has a stroke of 100 mm and a piston diameter of 16 mm. The cylinder has to be pressurized by an external pump.

B. Frame

In order for the prototype to work correctly the actuator must be placed in the middle of the prototype and have enough room to move around. As a direct result the frame is designed as an open box, see figure 14(b). Here the top part can be used to connect the prototype to for instance a robotic arm. The sides are used to connect the fingers. Note that the actuator is not directly connected to the frame. The bottom part of the frame is used similar to the palm of a hand, when grasping an object.

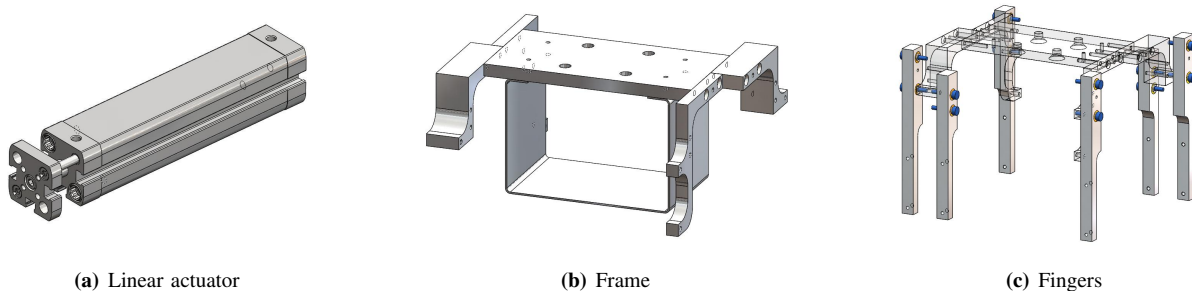


Figure 14. Parts of the prototype, including the linear actuator 14(a), the frame 14(b) which hold everything together and the six fingers which make contact with the object it is grasping. 14(c).

C. Fingers

The fingers are not placed optimally, especially because the finger in the middle had to be shifted to the side to make space for the actuator, as depicted in figure 14(c). Consequently the fingers on the outside had to make space for the finger in the middle and are therefore also moved a bit further out. As a result there are two pairs of fingers on either side of the gripper, where one finger is opposing two fingers. In the ideal situation one want to have each finger only opposing one other finger, which would have been the case if there was enough room in the middle of the prototype for the middle finger.

D. Parallelogram

The finger in the middle has to be connected to the side of the actuator that is located on the other side of the prototype. A parallelogram is used to transfer the motion from one side to the other, see figure 15(a). The part from which the motion is transferred by the parallelogram to the finger, is the revered to as the middle finger in the rest of the report, because the parallelogram and the actual finger are not modeled in the analysis, see appendix B.

E. Linkages

Each finger is connected to the actuator by a chain of linkages. Each chain contains of four linkages with five revolute joints, as depicted in figure 15(b). In the analysis the connection between the finger and the actuator was achieved by a single linkage which was connected by means of spherical joints. To make the prototype work the spherical joint for each linkage has to be positioned in the same position. Unfortunately it is not possible to place three spherical joints at the same location in reality. As a result the spherical joints were replaced by sets of revolute joints, of which the axis of rotation all intersect in the same position. This is indicated in figure 15(c) by the red sphere. On the other end, where the blue sphere is displayed, two revolute

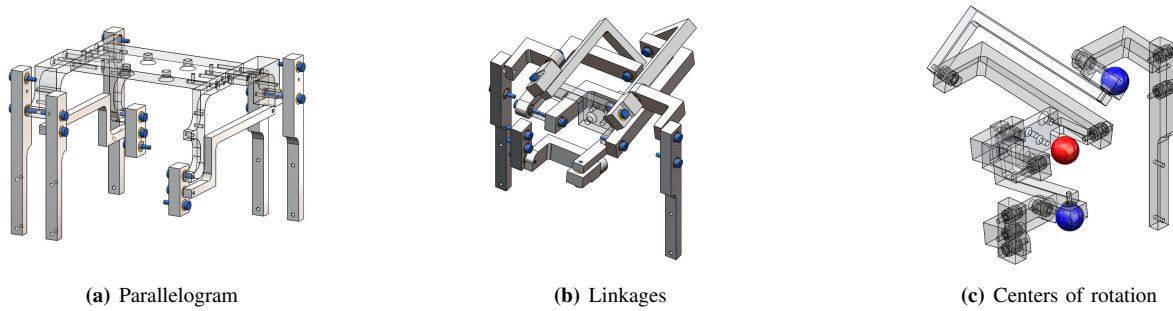


Figure 15. The parallelogram that is transferring the motion from one side of the prototype to the middle finger which is located on the other side, see 15(a), of the underactuated gripper with a floating differential actuator. The linkages connecting the fingers to the part which is bolted on the actuator is shown in figure 15(a). Note that the part which is bolted to the actuator is made transparent. The centers of rotation that result from the combinations of revolute joints in the chain of linkages, 15(c).

joints rotate around the same point such that it behaves as a cardan joint. Note that the linkages of the finger in the middle are most compact and the others are larger. This is because each set of linkages must be able to rotate around each other without blocking each other’s motions. To minimize friction in the system each joint is constructed with two ball bearings, see figure 16(a).

F. Prototype

Joining all the parts together result in the prototype as depicted in figure 17. The prototype is 0.371 m long and is 0.189 m wide. It can grasp objects up to a diameter of 0.130 m. and carry almost up to 4 kg for the objects with a smaller diameter. If all the fingers of the prototype are needed to grasp the object, then the object has to be at least 0.157 m long. The weight of the prototype is 0.7 kg.

G. Springs

During the initial tests of the prototype it became clear that the fingers could move independently from the actuator input as a result of the play in the prototype. This meant that springs had to be added to ensure that the fingers would return in the open grasp position. The springs are chosen such that their influence on the system is minimal, while maintaining enough force to keep the fingers in the open position when the actuator is completely contracted.

H. Loadcell

In case the actuation force of the actuator had to be measured an experimental setup is developed. Because the actuator needs to maintain its ability to move around freely it is essential to incorporate the possibility to place a loadcell in series with the linear actuator. This loadcell is compressed and therefore additional guidance is needed to prevent the loadcell from measuring forces other than the one in the direction of actuation. The design is modified to fit a load cell that can measure up to 111 N, see figure 16(c). The exact model is the FLLSB200 with stock number FSH00105 and made by Feteris Components.

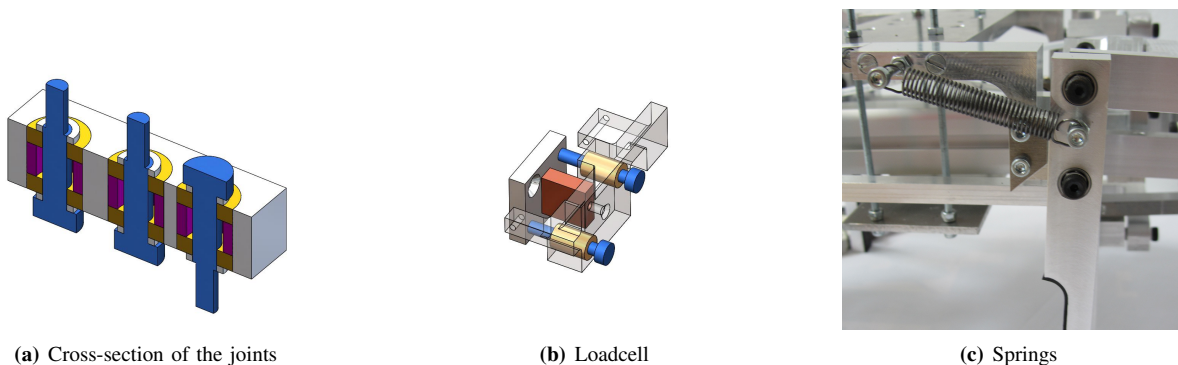
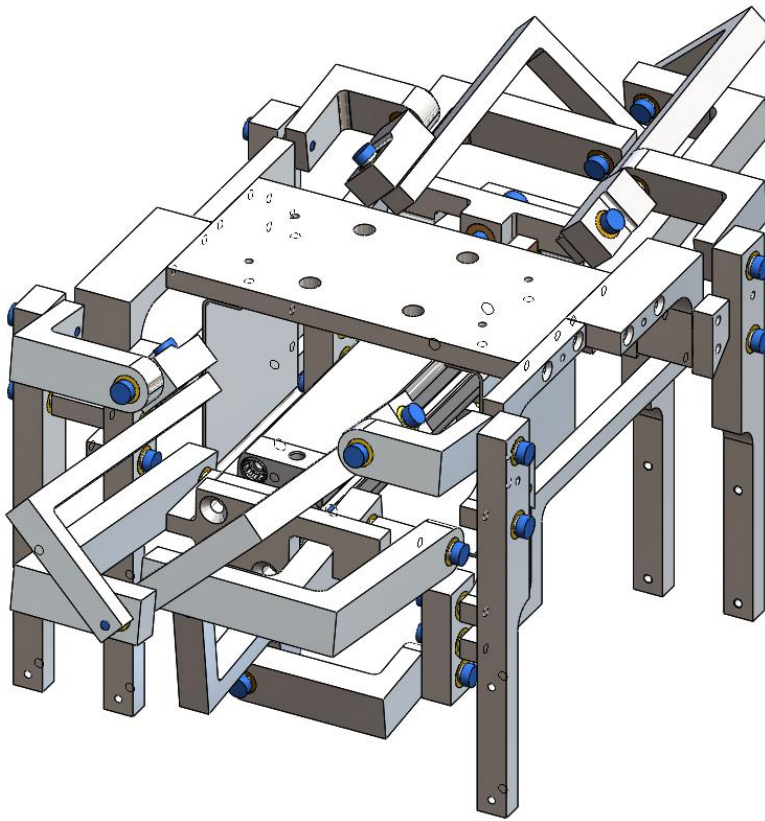
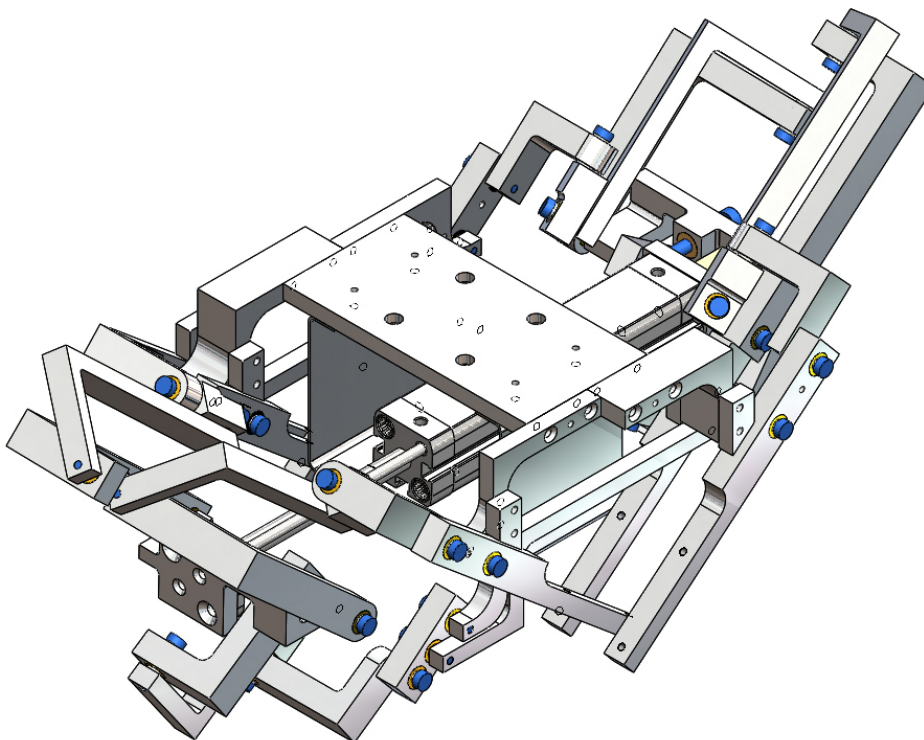


Figure 16. Figure 16(a) displays the cross-section of the revolute joints. Here the axle is the blue part and the ball bearings are yellow. The ball bearings are pinched by the axle, which is a bolt and are kept in place by a cylinder (purple), which is glued to the part. Figure 16(b) displays the setup for the loadcell (brown). To prevent other force, other than the measured, from acting on the loadcell guidance is put in place, which consist of two linear bearings (yellow). Figure 16(c) shows how the springs are spanned between the finger and the frame.



(a) Matlab model of the prototype in the open situation.

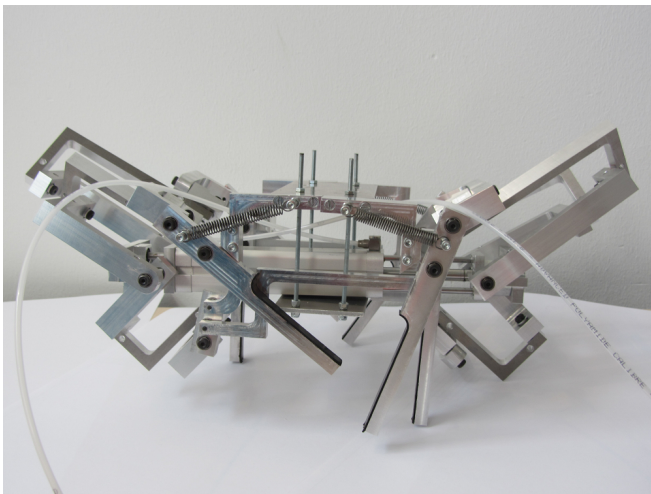


(b) Matlab model of the prototype in the closed situation.

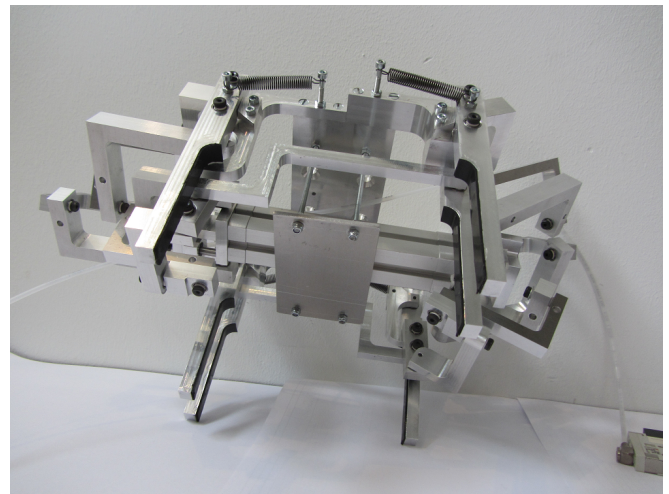
Figure 17. The prototype of the underactuated gripper with a floating differential actuator is shown in the fully open grasp position and the fully closed grasp position.

APPENDIX E
PHOTO GALLERY

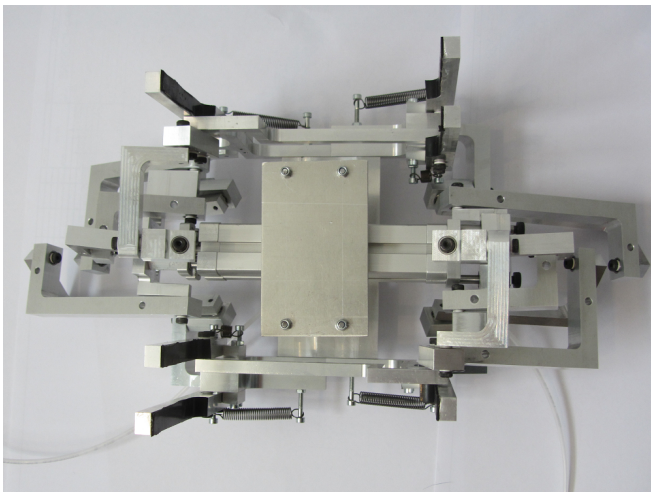
This section contains some nice photos from the prototype. These photos are not referred to in other sections of the report.



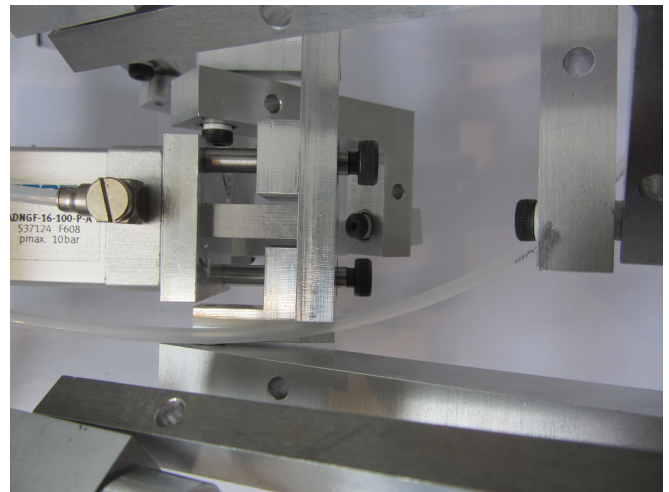
(a) Side view



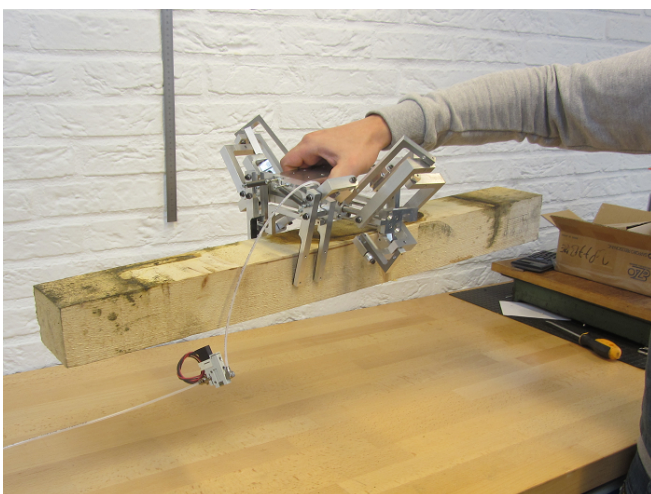
(b) Isometric bottom view



(c) Bottom view



(d) Detailed view of loadcell



(e) Holding a beam of 2.2 kg



(f) Holding a bottle of 1.2 kg

Figure 18. Six additional photos of the prototype